Chiral Indolylarylsulfone Non-Nucleoside Reverse Transcriptase Inhibitors as New Potent and Broad Spectrum anti-HIV-1 Agents

Valeria Famiglini,[†] Giuseppe La Regina,[†,*] Antonio Coluccia,[†] Domiziana Masci,[†] Andrea Brancale,[‡] Roger Badia,[∞] Eva Riveira-Muñoz,[∞] José A. Esté,[∞] Emmanuele Crespan,[§] Alessandro Brambilla,[§] Giovanni Maga,[§] Myriam Catalano,[+,ø] Cristina Limatola,[+,ø] Francesca Romana Formica,[°] Roberto Cirilli,[°] Ettore Novellino,[≠] and Romano Silvestri[†]

[†]Istituto Pasteur Italia - Fondazione Cenci Bolognetti, Dipartimento di Chimica e Tecnologie del Farmaco, Sapienza Università di Roma, Piazzale Aldo Moro 5, I-00185 Roma, Italy

[‡]Welsh School of Pharmacy, Cardiff University, King Edward VII Avenue, Cardiff, CF10 3NB, UK

[∞]AIDS Research Institute - IrsiCaixa, Hospitals Germans Trias i Pujol, Universitat Autonóma de Barcelona, 08916 Badalona, Spain

[§]Institute of Molecular Genetics IGM-CNR, National Research Council, via Abbiategrasso 207, I-27100 Pavia, Italy

[°]Dipartimento del Farmaco, Istituto Superiore di Sanità, Viale Regina Elena 299, I-00161 Roma, Italy

[+]Istituto Pasteur Italia - Fondazione Cenci Bolognetti, Dipartimento di Fisiologia e Farmacologia "Vittorio Erspamer", Sapienza Università di Roma, Piazzale Aldo Moro 5, I-00185 Roma, Italy

[ø]IRCCS Neuromed, Via Atinense 18, I-86077 Pozzilli, Italy

[≠]Dipartimento di Farmacia, Università di Napoli Federico II, Via Domenico Montesano 49, I-80131, Napoli, Italy

ABSTRACT

We designed and synthesized a series of chiral indolyarylsulfones (IASs) as new HIV-1 NNRTIs. The new IASs **8-37** showed potent inhibition of the HIV-1 WT NL4-3 strain and of the mutant K103N, Y181C, Y188L and K103N-Y181C HIV-1 strains. Six racemic mixtures, **8**, **23-25**, **31** and **33**, were separated at semipreparative level into their pure enantiomers. The (*R*)-**8** enantiomer bearing the chiral (α-methylbenzyl) was superior to the (*S*)-counterpart. IAS derivatives bearing the (*S*) alanine unit, (*S*)-**23,** (*S,R*)-**25**, (*S*)-**31** and (*S*)-**33**, were remarkably more potent than the corresponding (*R*)-enantiomers. Compound **23** protected hippocampal neuronal cells from the excitotoxic insult, while efavirenz (EFV) did not contrast the neurotoxic effect of glutamate. The present results highlight the chiral IASs as new NNRTIs with improved resistance profile against the mutant HIV-1 strains and reduced neurotoxic effects.

INTRODUCTION

Human immunodeficiency virus type 1 (HIV-1) is the etiological agent of the acquired immunodeficiency syndrome (AIDS), a serious health problem which globally affects more than 30 million people and caused about 1.1 million deaths in 2015.[1] Approved antiretroviral medicines include drugs falling in five main classes which target different steps of the viral life cycle: reverse transcription (nucleoside reverse transcriptase inhibitors (NRTIs), which also include the nucleotide agents, and non-nucleoside reverse transcriptase inhibitors (NNRTIs)), viral maturation inhibitors (protease inhibitors), viral entry (fusion inhibitors and co-receptor antagonists), and integration (integrase inhibitors). Antiretroviral therapy (ART) for the treatment of AIDS/HIV infection combines antiretroviral drugs targeting different steps of the HIV life cycle. At present, standard first-line ART for adults consists of two NRTIs plus a non-nucleoside reverse-transcriptase NNRTI or an integrase inhibitor.[2] The ART regimens have proven to control the HIV-1 replication and delay the progression of HIV infection, in particular in early stages of the disease. In most patients undergoing ART therapy the plasma viremia remains below the limit of detection for at least six months.[3] However, drug resistance and cross resistance, adverse side effects and toxicity problems leading to fail compliance, still remain pending problems of ART regimens.[4-6] Therefore, there is a considerable need for new anti-HIV drugs that show better profile against the predominant mechanism of resistance and improved tolerability.

Indolylarylsulfone (IAS) has proven to be a valuable scaffold for the design of potent HIV-1 NNRTIs. IASs bearing the 3',5'-dimethylphenylsulfonyl moiety at position 3 of the indole nucleus and different substituents (for example amino acid, hydroxyalkyl or Mannich base) at the indole-2-carboxamide nitrogen, e.g. **1** (type A, Chart 1), displayed inhibitory activities against wild-type (WT) and drug-resistant HIV-1 in nanomolar range.[7-11]

Efforts to overcome the problem of drug resistance led to the discovery of the second generation NNRTIs Etravirine (ETR) and Rilpivirine (RPV) which showed improved profile compared with the first generation NNRTIs.[12] The presence of three aromatic rings allow ETR and RPV to adopt variable binding conformations, which are minimally affected by mutations of the amino acid residues into the allosteric binding site of the NNRTIs.[13] Accordingly to this idea,[13,14] introduction of the third aromatic nucleus to the parent IAS compound provided NNRTIs, e.g. **2** (type B, Chart 1), with broad activity against the WT HIV-1 and the mutant K103N and Y181C HIV-1 strains.[15]

Asymmetric geometry of the HIV-1 non-nucleoside binding pocket, regiochemistry and stereochemistry of NNRTIs can dramatically influence their anti-HIV activity. Chiral HIV-1 NNRTIs are highly attractive since the enantiomers often show great differences of activity against the HIV-1 WT and the drug resistant mutant strains (for example, see Ref.s[16-19]). The effect of chirality on the activity of HIV-1 NNRTIs have been recently reviewed.[20] With respect to IAS, introduction of a methyl group at position α of the benzyl of **2** afforded (*R*)-**3** and (*S*)-**3** enantiomers (type B - chiral) which showed remarkably different activities against the K103N mutant HIV-1 strain: (*R*)-**3**, EC_{50} = 4.3 nM; (*S*)-**3**, EC_{50} =128 nM (Table 3).[21] On the contrary, the alanine enantiomers (*R*)-**4** and (*S*)-**4** (type A - chiral) showed much lower (5 times) difference of activity.[9] Replacement of the phenyl of **3** with a pyridin-4-yl ring provided compound **5**, with an even greater difference of activity.[22] The (*R*)-**5** enantiomer proved to be highly potent against HIV-1 WT, EC_{50} = 0.2 nM, K103N, EC_{50} = 0.2 nM, and Y181C, EC_{50} = 2.1 nM (Table 3).[22] Besides **5**, introduction of the pyrimidin-4-yl ring (**6**) or furan-2-yl (**7**) rings also led to potent anti-HIV-1 agents.[22] However, chemical modification of these substituents was not exhaustively explored. Herein, we designed and synthesized new IASs to explore structure-affinity relationships (SARs) of chiral units at the nitrogen of the indole-2-carboxamide. In particular, we report new IAS derivatives **8-37**, which exhibit potent anti-HIV-1 activity at low nano- and subnanomolar concentration (Chart 1 and Table 1). Contrary to previously reported results,[9] we found

that IAS derivatives bearing the (*S*)-alanine unit, **23**, **25**, **31** and **33** show high enantiospecific activity against HIV-1.

Chart 1. Structure of New IASs 8−37 and Reference Compounds 1−7.[a]

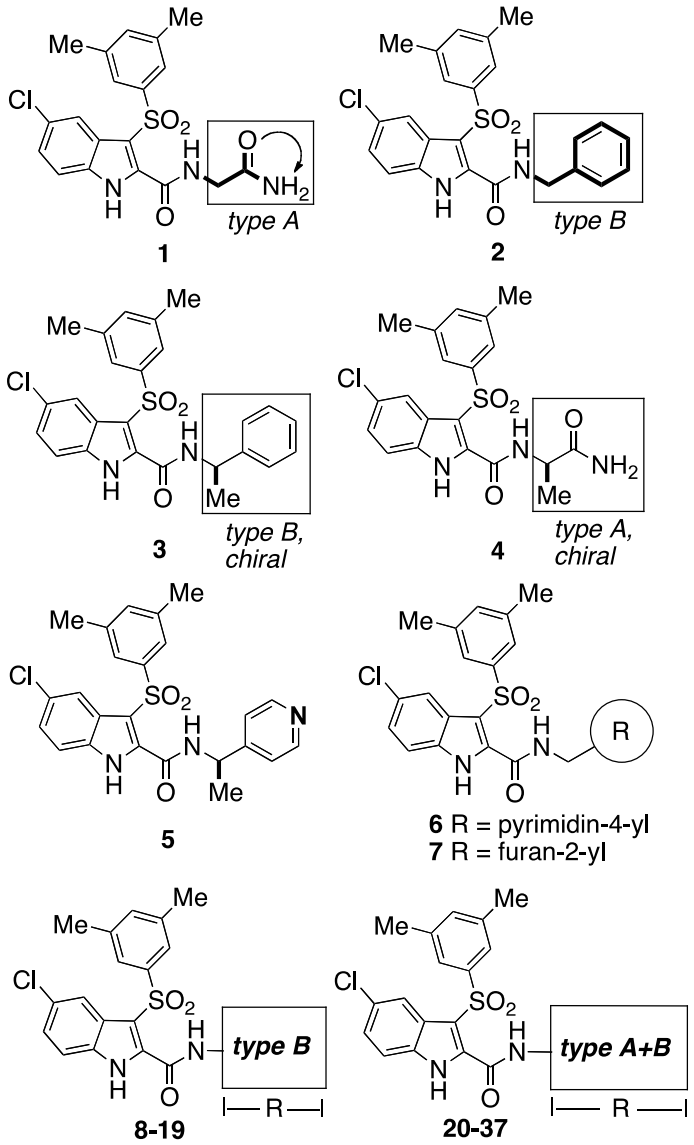

[a]**8−37**: see Table 1 for R substituent.

Despite significant progress, nearly half of people with HIV develop primary neurological conditions during ART treatment in both developed and undeveloped countries. There is an unmet need

of safer anti-HIV drugs for the long-term treatment of HIV infected people. The effect on damaged neurons of IAS **23**, a representative member of the IAS NNRTI class, was assessed by administration to hippocampal neuronal cultures in the presence of 100 μM glutamate as a neurotoxic stimulus. IAS **23** showed higher protective effect than EFV from the excitotoxicity.

CHEMISTRY

Carboxamides **8-14**, **18** and **19** were synthesized by coupling reaction of 5-chloro-3-((3,5-dimethylphenyl)sulfonyl)-1*H*-indole-2-carboxylic acid (**38**)[7] with the appropriate amine in the presence of benzotriazol-1-yl-oxytripyrrolidinophosphonium hexafluorophosphate (PyBOP reagent) and triethylamine in anhydrous DMF at 25 °C for 12 h. Alternatively, **38** was transformed into the corresponding acid chloride with oxalyl chloride and pyridine in anhydrous dichloromethane at room temperature for 2 h, or into carboxylic acid imidazolide with 1,1′-carbonyldiimidazole in anhydrous THF at 25 °C for 2 h. Subsequent treatment of the activated acid with the appropriate amine provided the carboxamides **15**-**17**. Compounds **20**-**37** were obtained under the same reaction conditions of carboxamides **8-14** and **17**-**19** starting from the corresponding acid **39**[8] or **40**[8] and the proper amine (Scheme 1).

Separations of the (*R,S*) racemic mixtures **8**, **23-25**, **31** and **33** were performed by enantioselective HPLC using polysaccharide-based chiral stationary phases (CSPs) and an appropriate CSP/eluent system (see Experimental section). After optimization of the analytical methods, semipreparative enantioseparations were set-up to obtain the pure enantiomers at milligram scale for screening. The absolute configurations of the enantiomers of **8, 23, 24, 31, 33** and four stereoisomers of **25** were empirically assigned by a combination of chemical correlation/enantioselective HPLC/circular

dichroism methods. Commercially available (*S*)-enantiomers of the amines were used as starting material for the stereospecific synthesis of the *(S)* forms. The enantiomeric excess of each enantiomer separated from the racemic mixtures **8**, **23-25**, **31** and **33** was determined by HPLC (Figures 5S-10S of Supporting Information).

Scheme 1. Synthesis of compounds **8**-**37.**[a]

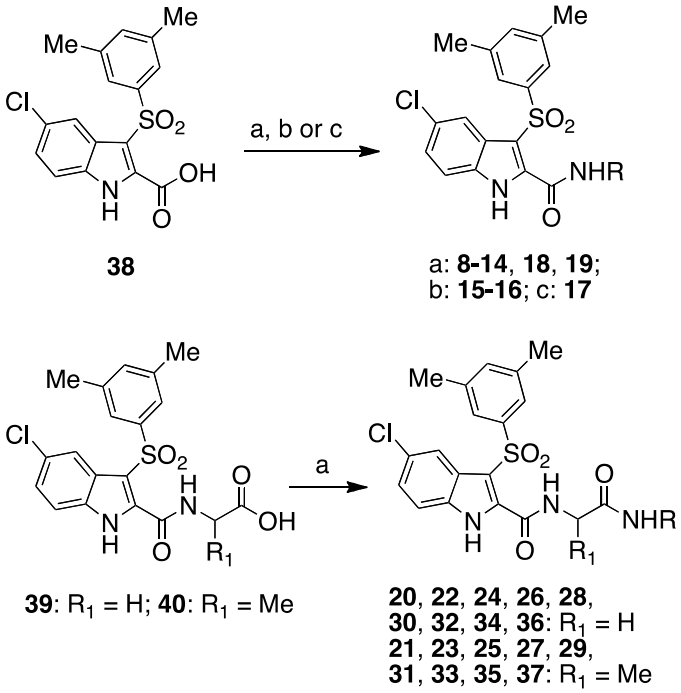

[a]Reagents and reaction conditions: (a) amine, PyBOP reagent, triethylamine, anhydrous DMF, 25 °C, 12 h, 35-98%; (b) (i) pyridine, oxalyl chloride, dichloromethane, 25 °C, 2 h, (ii) amine, 25 °C, 12 h, 7-11%; (c) (i) 1,1′-carbonyldiimidazole, anhydrous THF, 25 °C, 2 h, (ii) 3-(aminomethyl)aniline, 25 °C, 2 h, 71%.

RESULTS AND DISCUSSION

Anti-HIV-1 activity. The effective concentrations (EC_{50} values, nM) to inhibit by 50% the HIV-1 WT (NL4-3 strain) in MT-4 cells (MTT method), and cytotoxic concentrations (CC_{50} values, nM) to induce 50% death of non-infected cells of IASs **8-37** are shown in Table 1. Except compounds **10** (EC_{50} = 132.7 nM) and **26** (EC_{50} = 3.8 nM), all new IASs showed EC_{50} values at subnanomolar concentration, which were below the limit of detection of the assay. Compounds **8-15**, **17**, **19-22**, **24-26**, **28** and **30-36** displayed CC_{50} values >20000 nM, and **23**, **29** and **37** were in the 10000-20000 nM range. Several IASs showed selectivity indexes (SI = CC_{50}/EC_{50} ratio) >50000, three derivatives, **22**, **23** and **28**, SI>100000. IAS **22** showed the highest SI value (SI > 244620) within the series. The SI values were clearly superior to NVP, EFV, and ETR and comparable to the reference IASs **2-7**.

We initially synthesized IAS derivative **8-14** bearing different benzyl groups at the indole-2-carboxamide nitrogen. Introduction of a fluorine atom at position 2 of the phenyl group gave compound **8** that was as potent as **3** against the NL4-3 HIV-1 WT and superior to **3**, NVP and EFV against the mutant K103N (EC_{50} = 0.7 nM) and Y181C (EC_{50} = 103 nM) HIV-1 strains (Table 2). However, these values were slightly superior to those of compound **2**.[15] We separated at the semipreparative level the racemic mixture **8** into the pure enantiomers (*S*)-**8** and (*R*)-**8** by enantioselective HPLC on polysaccharide-based chiral stationary phases (CSPs). The (*S*)-**8** and (*R*)-**8** enantiomers proved to be equipotent (EC_{50} = 0.7 nM) against the NL4-3 HIV-1 WT strain and showed similar cytotoxicity (Table 3). Most importantly, the enantiomer (*R*)-**8** demonstrated potent antiretroviral activity against the mutant K103N and Y181C HIV-1 strains (EC_{50} = 0.7 nM) in the cellular assay, being 147-fold (K103N) and 871-fold (Y181C), respectively, more potent than (*S*)-**8**. Against the K103N and Y181C resistant mutants, (*R*)-**8** was more potent than reference drugs NVP, EFV and ETR. Also against recombinant HIV-1 RT carrying the K103N and Y181C mutations, *(R)*-**8** was several-fold more potent than *(S)*-**8** (Table 4).

Introduction of a methyl group at the methylene of IAS **7** gave **9** which except the Y181C (EC_{50} = 22 nM), showed modest inhibition of the mutant K103N, Y188L and K130N-Y181C HIV-1 strains (Table 2). The potent antiretroviral activity showed by **8** prompted the synthesis of fluoro-containing IAS derivatives **12-14**. Introduction of a fluorine atom at the α-methyl group of **3** afforded IAS **13**, a racemate that was superior to **3** against the K103N (EC_{50} = 0.7 nM) and Y181C (EC_{50} = 82 nM) HIV-1 resistance mutations, but did not inhibit the double mutant K130N-Y181C HIV-1 strain (Table 2). The 2,3-difluoro-IAS **14** proved to be potent inhibitor of the NL4-3 HIV-1 WT, and the mutant K103N (EC_{50} = 0.7 nM) and Y181C (EC_{50} = 2.0 nM) strains, but was ineffective against the double mutant K103N-Y181C strain (Table 2).

IASs **15** and **16** were designed as constrained analogues of **5** and **6**, where the nitrogen of the cyano group mimicked the nitrogen at position 1 of the pyridine/pyrimidine ring. Compound **15** proved to be a strong inhibitor of the K103N (EC_{50} = 0.6 nM) and Y181C (EC_{50} = 2.2 nM) HIV-1 mutations, but was unable to inhibit the double mutant K130N-Y181C strain. Extrusion of the basic nitrogen atom from the pyridinyl ring led to **17** and the structurally related derivatives **18** and **19**. The 3-aminobenzyl derivative **17** uniformly inhibited all HIV-1 strains: NL4-3 WT, K103N and Y181C, EC_{50} = 0.7 nM; Y188L, EC_{50} = 24 nM and K103N-Y181C, EC_{50} = 86 nM. Incorporation of the 3-amino group into a 2-aminoimidazolyl moiety (compound **18**) caused considerable decrease of activity against all viral strains and recombinant HIV-1 RT (Table 2 and Table 5). On the contrary, the indazol-3-yl derivative **19** inhibited the NL4-3 HIV-1 WT and the mutant K103N and Y181C strains with EC_{50} = 0.6 nM, and showed significant inhibition of the Y188L and K103N-Y181C strains with EC_{50} of 142 nM and 548 nM, respectively (Table 2).

Table 1. Anti-HIV-1 Activity of IASs 8-37, Reference Compounds 2, 3, 5-7, and NVP, EFV, ETR and AZT against HIV-1 NL4-3 Strain.[a,b]

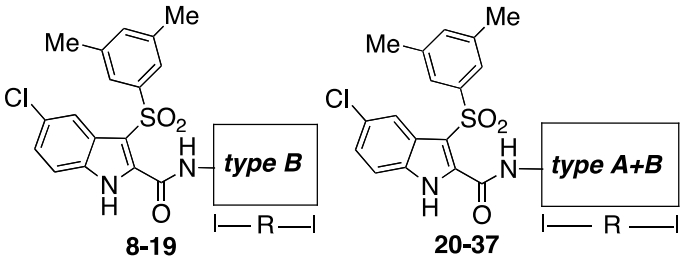

compd	R	HIV-1 NL4-3		
		CC_{50}[b] (nM)	EC_{50}[c] ± SD (nM)	SI[d]
8[f]		>51545	0.7[e]	>73642
9[f]		>54711	0.7[e]	>78159
10[f]	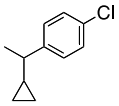	>47397	132.7 ± 12	>359
11	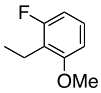	>49903	0.6[e]	>83172
12[f]	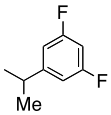	>49706	0.6[e]	>82842
13[f]		49178 ± 4103	0.7[e]	>70255
14		>51132	0.7[e]	>73046
15	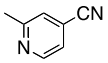	>53773	0.6[e]	>89621
16	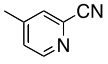	6840 ± 1420	0.7[e]	>9771
17	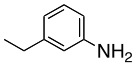	>53422	0.7[e]	>76317

18	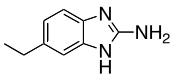	5886 ± 335	0.6[e]	>9810
19	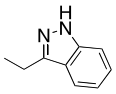	>50711 ± 0	0.6[e]	>84518
20[f]	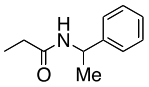	29387 ± 8	0.6[e]	>48978
21[f]	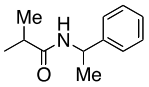	21745 ± 5626	0.6[e]	>36856
22	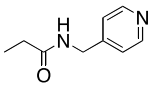	>48924	0.2[e]	>244620
23[f]	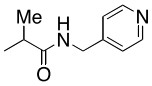	19465	0.2[e]	102452
24[f]	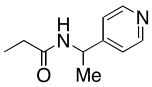	47045 ± 762	0.6[e]	>78408
25[f]	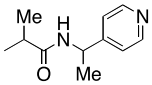	21890 ± 557	0.6[e]	>36483
26	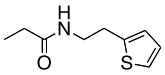	35730	3.8 ± 2.1	9478
27[f]	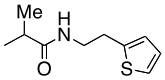	9502	0.2[e]	52789
28	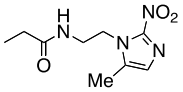	24466	0.2[e]	143922
29[f]	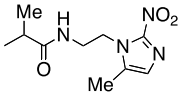	16012	0.2[e]	94188
30	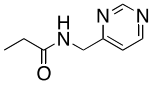	>48830	0.6[e]	>81383
31[f]	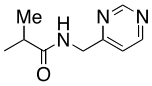	28068 ± 2083	0.6[e]	>46780
32	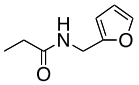	>50043	0.6[e]	>83405
33[f]	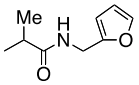	24241 ± 9687	0.6[e]	>40402

34	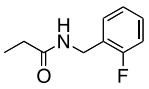	>47349	0.6[e]	>78916
35[f]	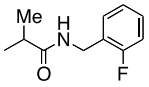	23265 ± 7343	0.6[e]	23265
36[f]	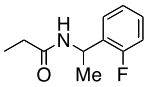	23007 ± 4908	0.6[e]	>38345
37[f]	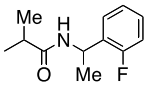	15232 ± 199	0.6[e]	>25387
2[g]		37994 ± 12164	0.2[e]	172700
3[f,h]		>53535	0.6[e]	>205903
5[f,i]		30216 ± 2308	0.2 ± 0.2	151078
6[i]		>54953	0.22[e]	>249786
7[i]		>56433	0.2 ± 0.1	>282218
NVP[j]	—	>18776	112.4 ± 74.9	>167
EFV[k]	—	>15839	15.9 ± 12.7	>996
ETR[l]	—	>22973	16.1 ± 14.2	>1426
AZT[m]	—	>30595	3.7 ± 3.7	>8269

[a]Data are mean values of two to three independent experiments each one in triplicate. [b]CC_{50}: cytotoxic concentration (nM) to induce 50% death of noninfected cells, as evaluated with the MTT method in MT-4 cells. [c]EC_{50} (HIV-1 NL4−3): effective concentration (nM) to inhibit by 50% HIV-1 (NL4−3 strain) induced cell death, as evaluated with the MTT method in MT-4 cells. [d]SI: selectivity index calculated as CC_{50}/EC_{50} ratio. [e]Lowest detectable nM concentration. [f]Data of the racemic mixture. [g]Lit.[15] [h]Lit.[16] [i]Lit.[22] [j]NVP, nevirapine. [k]EFV, Efavirenz. [l]ETR, etravirine. [m]AZT, azidothymidine.

We synthesized IASs **20-25** by coupling a type A unit, the amino acid glycine (**1**) or alanine (**4**), with a type B unit, the benzyl of **2**, the α-methylbenzyl of **3** or the 1-(pyridin-4-yl)ethyl group of **5**. All compounds strongly inhibited the WT NL4-3 HIV-1 strain. Racemic compounds **21**, **23** and **25**, bearing the alanine unit inhibited the mutant K103N HIV-1 strain at nanomolar concentrations with EC_{50} values of 1.9, 1.9 and 7.4 nM, respectively (Table 2). On the other hand, compound **22** and racemates **23** and **24** bearing the (pyridin-4-yl) group as a terminal tail showed potent inhibition of the mutant Y181C HIV-1 strain with EC_{50} values of 20, 21 and 0.6 nM, respectively. Compound **23** and **24** inhibited the mutant K103N-Y181C and Y188L HIV-1 strains with of EC_{50} = 838 nM and EC_{50} = 610 nM, respectively.

The racemic mixtures **23** and **24** were resolved at the semipreparative level by enantioselective HPLC into the corresponding pure enantiomers (*R*)-**23**, (*S*)-**23**, and (*R*)-**24**, (*S*)-**24**; the diastereomeric mixture **25** was separated into the four stereoisomers (*R,S*)-**25**, (*S,R*)-**25**, (*R,R*)-**25** and (*S,S*)-**25** (Table 3). Enantiomers (*R*)-**23** and (*S*)-**23** proved to be equipotent (EC_{50} = 0.7 nM) against the NL4-3 HIV-1 WT; however, (*S*)-**23** was remarkably superior to (*R*)-**23** against the mutant K103N (EC_{50} = 0.7 nM, 162-fold), Y181C (EC_{50} = 0.7 nM, 258-fold), Y188L (EC_{50} = 666 nM, >35-fold) and K103N-Y181C (EC_{50} = 857 nM, 8-fold) HIV-1 strains. Similar results were obtained against the corresponding mutated HIV-1 RT enzymes (Table 4). Enantiomers (*R*)-**24** and (*S*)-**24** showed small differences of activity against all HIV-1 mutants. IAS derivatives (*R,S*)-**25** and (*S,R*)-**25** showed significant differences: (*S,R*)-**25** was 3-fold (WT, EC_{50} = 0.6 nM), 340-fold (K103N, EC_{50} = 0.6 nM), 1113-fold (Y181C, EC_{50} = 0.6 nM), 38-fold (Y188L, EC_{50} = 742 nM) and 15-fold (K103N−Y181C, EC_{50} = 1261 nM), respectively, more potent than (*R,S*)-**25** in the cellular assay; (*S,S*)-**25** was superior to (*R,R*)-**25** against the NL4-3 WT (EC_{50} = 0.6 nM, 6-fold), K103N (EC_{50} = 1.3 nM, 927-fold), Y181C (EC_{50} = 0.6 nM, 1948-fold), Y188L (EC_{50} = 612 nM, 44-fold) and K103N-Y181C (EC_{50} = 1280 nM, 21-fold). The cellular activity of the enantiomers **25** correlated with the enzymatic data (Table 4).

Table 2. Activity of Compounds 8-37, Reference Compounds 2, 3, 5-7, and NVP, EFV, ETR and AZT against Mutant HIV-1 Strains.[a,b]

	EC_{50} (nM)			
compd	**K103N**	**Y181C**	**Y188L**	**K103N-Y181C**
8[f]	0.7[c] 1[d]	103 ± 6 >147	969 ± 680 >1384	3959 ± 1253 >5656
9[f]	109 ± 22 155	22 ± 4.4 31	350 ± 160 500	12037 ± 11489 17195
10[f]	nd[e]	nd	nd	nd
11	0.6 1	399 ± 39 665	nd	27746 ± 31339 46243
12[f]	1.2 ± 0.8 2	716 ± 179 1198	nd	>49706 >82843
13[f]	0.7 1	82 ± 62 117	nd	27321 ± 34270 39030
14	0.7 1	2.0 ± 2.0 2.9	nd	>51132 >73046
15	0.6 1	2.2 ± 0.7 3.7	nd	>53773 >89622
16	0.7 1	65 ± 22 92	nd	>6840 >9771
17	0.7 1	0.7 1	24 ± 8.7 34	86 ± 107 123
18	18 ± 20 30	79 ± 59 132	nd	>5886 >9810
19	0.6 1	0.6 1	142 ± 101 237	548 ± 12 913
20[f]	210 ± 19 350	76 ± 76 127	1622 ± 1278 2703	>29387 >48978
21[f]	1.9 ± 3.7 3.2	167 ± 67 283	3792 ± 780 6427	24868 ± 6440 42149
22	190 ± 12 316	20 ± 6 100	1401 ± 72 700	6086 ± 206 30430
23[f]	1.9 ± 0.2 52	21 ± 8 105	819 ± 221 4095	838 ± 21 4190

24[f]	38 ± 19 64	0.6 1	610 ± 38 1017	13333 ± 13752 22227
25[f]	7.4 ± 0.4 12	167 ± 74 278	12893 ± 13226 21488	>36483 >60805
26	1340 ± 652 352	321 ± 112 84	>3576 >941	>3576 >941
27[f]	18 ± 0.9 30	129 ± 54 215	>9802 >16336	>9802 >16336
28	279 ± 124 1395	17 ± 11 85	2321 ± 815 11605	4677 ± 2012 23285
29[f]	170 ± 115 850	170 ± 84 850	4770 ± 2118 23850	5281 ± 2021 26405
30	19.6 ± 19.6 33	0.6 1	449 ± 27 >743	2305 ± 2500 >3842
31[f]	0.6 1	0.6 1	760 ± 95 >1267	798 ± 456 >1330
32	60 ± 80 >86	<0.6 nd	1120 ± 500 >1600	18534 ± 21570 >26477
33[f]	1.9 ± 1 3	27 ± 3.9 45	2432 ± 972 4053	4513 ± 2015 >7521
34	1326 ± 1288 1894	1.3 ± 1.5 1.9	6155 ± 3863 10258	>47349 >72248
35[f]	26 ± 1.9 43	93 ± 56 155	4240 ± 2015 7067	>23265 >38775
36[f]	387 ± 239 552	13 ± 7.4 19	3671 ± 110 6118	>23007 >38345
37[f]	36 ± 36 6	108 ± 77 180	>15232 >25387	6474 ± 3156 10790
2[g]	0.9 ± 0.4 4	18 ± 7.0 80	90 ± 83 409	1921 ± 2050 8691
3[f,h]	33 ± 6.4 55	720 ± 690 1200	nd	3267 ± SD 5445
5[f,i]	9.4 ± 2.3 47	87 ± 75 435	nd	1111 ± 940 5555
6[i]	0.22[d] 1	2.20 ± 1.3 10	50.6 ± 21.9 257	132 ± 153 600
7[i]	0.2[d] 1	0.8 ± 0.2 4	45 ± 0.23 225	971 ± 474 4855

NVP	>3756 >33	>3756 >33	>3756 >33	>3756 >33
EFV	130 ± 180 8.2	160 ± 180 10	760 ± 630 48	>317 >20
ETR	0.7 ± 0.4 0.04	18 ± 14 1.1	16 ± 9 1	4.6 ± 2 0.2
AZT	16 ± 12 4.3	6.0 ± 3.4 1.6	33 ± 18 8.9	16 ± 13 1.0

[a]Data are mean values of two to three independent experiments each one in triplicate. [b]EC_{50}: effective concentration (nM) to inhibit by 50% cell death induced by the indicated mutant HIV-1 strain, as evaluated with the MTT method in MT-4 cells. [c]Lowest detectable nM concentration. [d]FC: fold change obtained as ratio between EC_{50}s of the indicated drug resistant mutant HIV-1 strain and HIV-1 WT NL4-3 strain. [e]nd: no data. [f]Data of the racemic mixture. [g]Lit.[15] [h]Lit.[16] [i]Lit.[22]

In the cellular assay, the (*R*)-enantiomer of IAS derivatives bearing a single type B unit was superior to the (*S*)-counterpart (compare (*R*)-**8** with (*S*)-**8**, (*R*)-**3** with (*S*)-**3**,[21] and (*R*)-**5** with (*S*)-**5**[22]) (Table 3). In previous studies, the chirality of the alanine only weakly affected the antiretroviral activity (e.g.: **4**: single type A unit).[9] On the contrary, coupling of alanine with pyridin-4-ylmethanamine (type A+B, chiral) resulted in high stereospecific activity: (*S*)-**23** was superior to the corresponding (*R*)-enantiomer, and (*S,R*)-**25** and (*S,S*)-**25** were superior to the corresponding (*R,S*)-**25** and (*R,R*)-**25** enantiomers. To confirm these observations, we separated racemates **31** and **33** having the chiral alanine. As inhibitors of the HIV-1, the (*S*) enantiomers of these chiral derivatives, (*S*)-**31** and (*S*)-**33**, proved to be more potent than their (*R)* counterparts (Table 3).

Table 3. Anti-HIV-1 Activity of Racemates 8, 23-25, 31, 33, Reference Compounds 3, 5, and the corresponding Enantiomers against Mutant HIV-1 Strains.[a,b]

	EC_{50} (nM)				
compd	**WT**	**K103N**	**Y181C**	**Y188L**	**K103N-Y181C**
8[g]	0.7[c]	0.7[c]	103 ± 6	969 ± 680	3959 ± 1253
(R)-**8**	0.7[c]	0.7[c]	0.7[c]	165 ± 21	2486 ± 2743
(S)-**8**	0.7[c]	103 ± 8	680 ± 432	>51551	>51551
23[g]	0.2[c]	1.9 ± 0.6	21 ± 9	819 ± 315	838 ± 215
(R)-**23**	0.7[c]	114 ± 4	181 ± 38	>23104	7123 ± 2324
(S)-**23**	0.7[c]	0.7[c]	0.7[c]	666 ± 38	857 ± 723
24[g]	0.6[c]	305 ± 95	11.2 ± 4	610 ± 38	13333 ± 13752
(S)-**24**	0.7[c]	438 ± 229	2.5 ± 3	3048 ± 114	4628 ± 1581
(R)-**24**	0.7[c]	152 ± 38	5.71 ± 2	3272 ± 818	12246 ± 171
25[g]	0.6[c]	7.4 ± 0.4	167 ± 74	12893 ± 13226	>364
(R,S)-**25**	1.9 ± 0.4	204 ± 37	668 ± 37	>28532	19348 ± 14246
(S,R)-**25**	0.6[c]	0.6[c]	0.6[c]	742 ± 260	1261 ± 612
(S,S)-**25**	0.6[c]	1.3 ± 1.1	0.6[c]	612 ± 202	1280 ± 556
(R,R)-**25**	3.8 ± 0.2	1206 ± 111	1169 ± 779	>27010	>27010
31[g]	0.6[c]	0.6[c]	0.6 [c]	760 ± 95	798 ± 456

(R)-**31**	0.6[c]	76 ± 76	171 ± 57	5738 ± 1748	>24543
(S)-**31**	0.6[c]	0.6[c]	0.6[c]	380 ± 128	779 ± 532
33[g]	0.6[c]	1.9 ± 1	27 ± 3.9	2432 ± 972	4513 ± 2115
(R)-**33**	0.6[c]	311 ± 123	933 ± 369	>30195	>30195
(S)-**33**	0.6[c]	0.6[c]	3.5 ± 3.9	700 ± 175	1886 ± 715
3[e,g]	0.6[c]	33 ± 6.4	720 ± 690	nd[d]	3267 ± SD
(R)-**3**[e]	2.1 ± 1.9	4.3 ± 3.2	86 ± 43	193 ± 64	nd
(S)-**3**[e]	6.3 ± 4.2	128 ± 107	3469 ± 1735	>36404	nd
5[f,g]	0.2[c]	9.4 ± 2.3	87 ± 75	nd	1111 ± 453
(R)-**5**[f]	0.2[c]	0.2[c]	2.1 ± 1.5	933 ± 2.3	150 ± 17
(S)-**5**[f]	0.2[c]	4.3 ± 1.7	128 ± 11	5169 ± 3160	4124 ± 913
NVP	112.4 ± 74.9	>3756	>3756	>3756	>3756
EFV	15.9 ± 12.7	130 ± 180	160 ± 180	760 ± 630	>317
ETR	16.1 ± 14.2	0.7 ± 0.4	18 ± 14	16 ± 9	4.6 ± 2
AZT	3.7 ± 3.7	16 ± 12	6.0 ± 3.4	33 ± 18	16 ± 13

[a]Data are mean values of two to three independent experiments each one in triplicate. [b]EC_{50}: effective concentration (nM) to inhibit by 50% cell death induced by the indicated mutant HIV-1 strain, as evaluated with the MTT method in MT-4 cells. [c]Lowest detectable nM concentration. [d]nd, not done. [e]Lit.[21] [f]Lit.[22] [g]Data of the racemic mixture.

Table 4. Anti-HIV-1 Activity of pure Enantiomers of 8, 23, 25, 31, 33, and NVP, EFV and ETR against the WT RT, K103N, Y181I and K103N-Y181C Mutant RTs.[a]

	IC_{50} (nM)[b]			
compd	**WT**	**K103N**	**Y181I**	**K103N-Y181C**
(R)-**8**	87 ± 7	228 ± 21	456 ± 52	222 ± 19
(S)-**8**	175 ± 11	nd[c]	17220 ± 1214	>10000
(R)-**23**	13010 ± 3000	>50000	60980 ± 3214	>200000
(S)-**23**	506 ± 74	417 ± 64	870 ± 52	>40000
(R,S)-**25**	1190 ± 74	3550 ± 780	9510 ± 1123	8420 ± 950
(S,R)-**25**	610 ± 85	300 ± 67	1700 ± 112	490 ± 88
(S,S)-**25**	430 ± 28	2590 ± 800	440 ± 61	860 ± 120
(R,R)-**25**	410 ± 52	23700 ± 5000	5790 ± 622	13800 ± 1900
(R)-**31**	1800 ± 250	19910 ± 380	3350 ± 262	nd
(S)-**31**	470 ± 63	2860 ± 420	3140 ± 168	14280 ± 2000
(R)-**33**	145 ± 25	70 ± 9	276 ± 18	233 ± 33
(S)-**33**	113 ± 11	1120 ± 250	14210 ± 915	9640 ± 1200
NVP	400 ± 36	7000 ± 690	>20000	nd
EFV	80 ± 7	>20000	400 ± 22	nd
ETR	10 ± 0.5	20 ± 3	164 ± 15	97 ± 11

[a]Data are the mean values of at least three separate experiments. [b]Compound concentration (IC_{50}, nM) required to inhibit the RT activity of the indicated strain by 50%. [c]nd: no data.

Table 5. Anti-HIV-1 Activity of Compounds 16-18, 30, 32, and NVP, EFV and ETR against the WT RT, K103N, Y181I and K103N-Y181C Mutant RTs.[a]

	IC_{50} (nM)[b]			
compd	**WT**	**K103N**	**Y181I**	**K103N-Y181C**
16	23 ± 3	72 ± 11	306 ± 49	514 ± 102
17	41 ± 7	66 ± 11	64 ± 10	35 ± 5
18	278 ± 44	183 ± 27	284 ± 49	470 ± 70
30	202 ± 37	548 ± 93	529 ± 99	835 ± 110
32	145 ± 20	538 ± 93	461 ± 461	586 ± 85
NVP	400 ± 36	7000 ± 690	>20000	nd[c]
EFV	80 ± 7	>20000	400 ± 22	nd
ETR	10 ± 0.5	20 ± 3	164 ± 15	97 ± 11

[a]Data are the mean values of at least three separate experiments. [b]Compound concentration (IC_{50}, nM) required to inhibit the RT activity of the indicated strain by 50%. [c]nd: no data.

The inhibitory concentrations (IC_{50} values, nM) to inhibit by 50% the HIV-1 WT RT and the K103N, Y181I and K103N-Y181C mutated RTs are depicted in Tables 4 and 5. Among the tested compounds, eutomers, *(R)*-**8**, *(S)*-**23**, *(S,R)*-**25,** *(S,S)*-**25** (except Y181I), *(R)*-**33,** and compounds **16-18** inhibited the HIV-1 WT RT and the K103N and Y181C mutated RTs with IC_{50} values at high nanomolar concentration. Compounds *(R)*-**8**, **16-18**, *(S,R)*-**25***, (S,S)*-**25**, **30, 32** and *(R)*-**33** inhibited the HIV-1 K103N-Y181C mutated RT in the same range of concentration. In general, antiviral data in cell

cultures correlated with inhibitory enzymes data. Enantiomers with the highest inhibition of HIV-1 WT and mutant strains in MT-4 cells showed the best inhibition of HIV-1 WT and mutated RTs (compare cellular and enzymatic data of *(R)*-**8** with *(S)*-**8**, *(R)*-**23** with *(S)*-**23**, *(R,S)*-**25** with *(S,R)*-**25,** *(R,R)*-**25** and *(S,S)*-**25**, *(R)*-**31** with *(S)*-**31**. (Tables 1-5). In MT-4 cells, compound *(R)*-**8** inhibited the HIV-1 WT and the K103N and Y181C mutant strains with EC_{50} of 0.7 nM (Tables 1 and 2), and the corresponding RTs with IC_{50}s of 87, 228 and 456 nM (Table 4), respectively. Compound **17** showed the same EC_{50} values against HIV-1 WT, K103N and Y181C strains in MT-4 cells (Tables 1 and 2), and inhibited the corresponding RTs with IC_{50}s of 41, 66 and 64 nM, respectively (Table 5). Interestingly, in MT-4 cells, **17** potently inhibited the HIV-1 K103N-Y181C double mutant with EC_{50} of 86 nM (Table 2) and the corresponding RT with IC_{50} of 35 nM (Table 5). IAS derivative (*S,R*)-**25** inhibited the HIV-1 WT and the K103N and Y181C mutant strains with EC_{50}s of 0.6 nM, and the HIV-1 K103N-Y181C with EC_{50} of 1261 nM (Table 3). For comparison, *(R,S)*-**25** showed notably higher inhibitory concentrations in both cellular and enzymatic assays.

Molecular modeling. The binding mode of the reported compounds was evaluated by a series of molecular docking simulations using a previously reported procedure.[13] The docking results showed consistent binding modes in the HIV-1 WT RT as well as in the mutated K103N, Y181C and K103N-Y181C RTs. The key interactions observed are: (i) a H-bond between the indole NH and the K101 carbonyl oxygen; (ii) the chlorine atom fitted into a hydrophobic cavity near V106 and L234; (iii) the 3,5-dimethylphenyl moiety placed in the aromatic cleft formed by the side chains of Y181, Y188, and W229; (iv) a series of hydrophobic interactions between the linker and the heteroaryl moieties with the side chains of V179 and E138:B. The reported binding mode, in accordance with the biological data, was consistent between the enantiomeric couples. The binding modes of derivatives (*R*)-**8** and (*S*)-**8** proposed by *PLANTS* are shown in Figure 1.

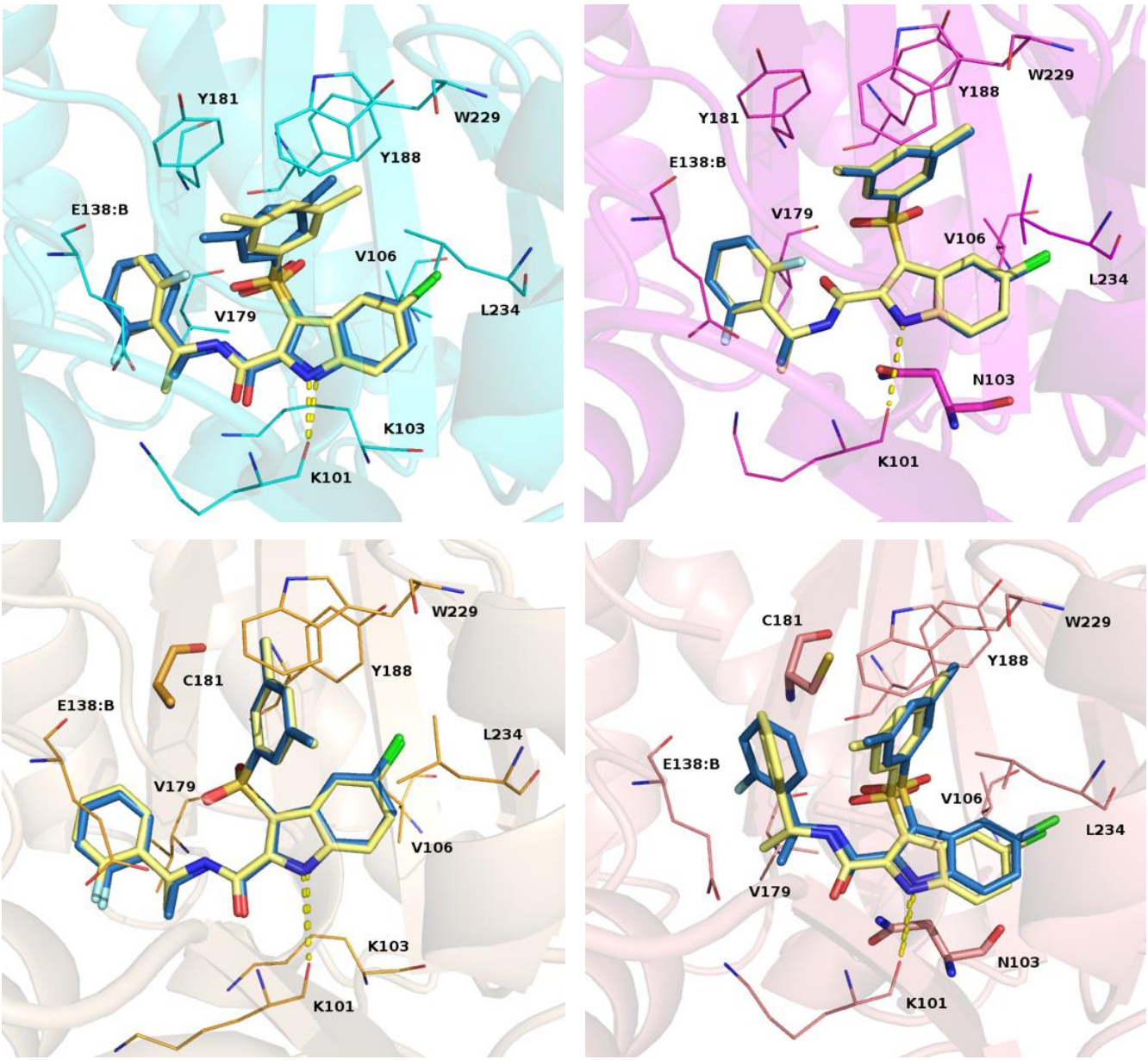

Figure 1. *PLANTS* proposed binding modes for derivatives (*R*)-**8** (yellow) and (*S*)-**8** (blue) into the non-nucleoside binding site of the RT: top left panel, WT (cyan); top right panel, K103N (magenta); bottom left panel, Y181C (orange); bottom right panel, K103N-Y181C (pink). Residues involved in interactions are reported as lines. Mutated residues are depicted as stick. RTs are shown as cartoon. H-bonds are depicted as yellow dotted lines.

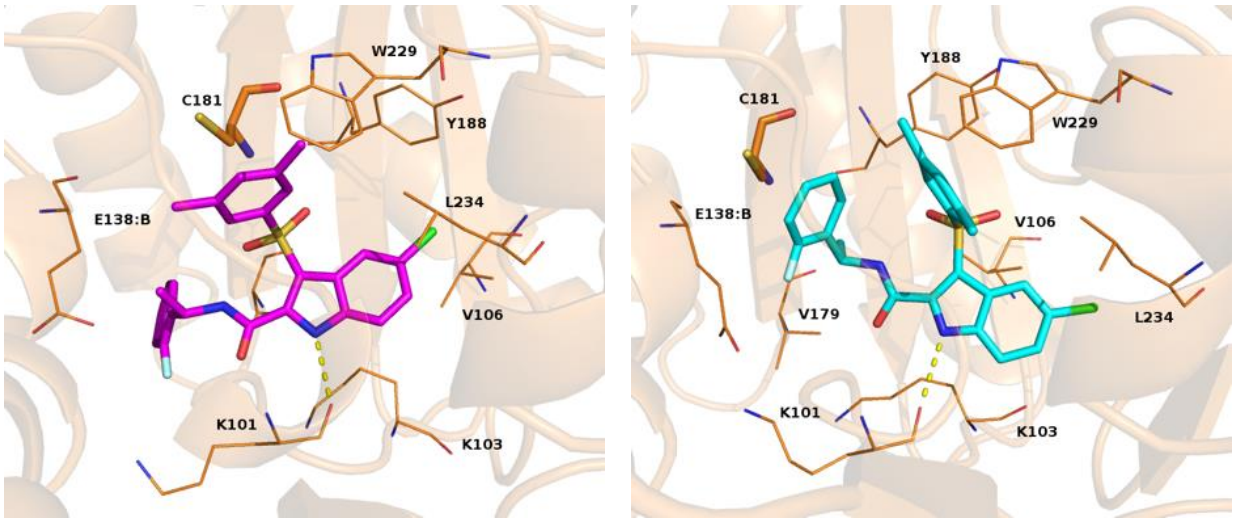

Figure 2. Trajectories snapshots versus the Y181C RT: left panel, (*S*)-**8** (magenta); right panel, (*R*)-**8** (cyan). Residues involved in interactions are reported as lines. Mutated residue is depicted as stick. RT is shown as cartoon. H-bonds are depicted as yellow dotted lines.

Interestingly, the biological results showed specific correlation between the linker length and the configuration of the asymmetric center: the most active enantiomer of IASs bearing the short linker (chiral type B) unit was generally in the (*R)* configuration, while the (*S)* enantiomer was superior in the longer linker (chiral type A unit) series. To gain further insight of the different behavior of the various enantiomers, we carried out a series of molecular dynamic simulations of two representative pairs of derivatives: (*R*)-**8**, (*S*)**-8** (short linker) and (*R*)-**23**, (*S*)-**23** (long linker). We used the Y181C mutated RT in the simulations because of the greatest differences of IC_{50} values within the enantiomeric pairs.

In comparing the trajectories of the (*R*)-**8** and (*S*)-**8**/Y181C RT complexes, the breakage of the interaction between the dimethylphenyl moiety of (*R*)-**8** and Y181 was compensated by the new interaction between the fluorinated aromatic ring and the C181 residue.[23] (Figure 2). Furthermore, the asymmetric methyl group was positioned into a hydrophobic cleft located toward the inner part of the binding pocket formed by V179, C181 and Y188 residues. With (*S*)-**8,** the methyl moved far from above indicated hydrophobic residues and thus failed these key interactions. The other contacts observed in the docking studies were retained during the whole simulations by both enantiomers (Figure 2).

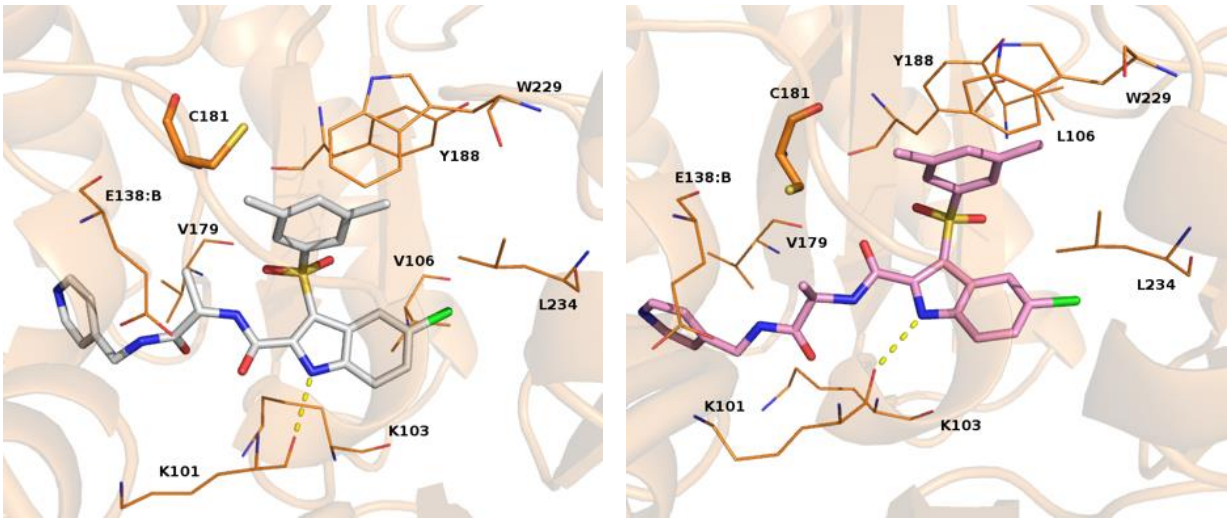

Figure 3. Trajectories snapshots versus K103N RT: left panel, (*S*)-**23** (white); right panel, (*R*)-**23** (pink). Residues involved in interactions are reported as lines. Mutated residue is depicted as stick. RT is shown as cartoon. H-bonds are depicted as yellow dotted lines.

A similar behavior was observed in the trajectories of (*R*)-**23** and (*S*)-**23**/Y181C RT complexes. The (*S*) asymmetric methyl group laid in the V179, C181 and Y188 cleft forming hydrophobic contacts, while the (*R*) methyl did not. For both (*R*)-**23** and (*S*)-**23** enantiomers the dimethylphenyl group was stabilized by interaction with C181 and the pyridine ring, due to the longer linker, formed contact with E138:B (Figure 3).

The simulations confirmed the crucial role of the linker. Indeed, the enantiomer with the best antiviral activity shifted from (*R*) to (*S*) moving from short to long linker because of its best fitting at the binding site. (Figure 1S, Supporting Information). The correlation between the calculated binding free energy for four compounds with the experimental IC_{50} (r^2 of 0.75) supports the proposed structural binding model (Table 6).

Table 6. Experimental IC_{50} versus computed binding free energy.

Comp	Exp. Y181C IC_{50}	Calc. ΔG
(*R*)-**8**	0.456	-9.876
(*S*)-**8**	17.22	-9.279
(*R*)-**23**	60.98	-9.135
(*S*)-**23**	0.87	-9.731

Neurotoxicity studies. ART has significantly increased life expectancy of HIV infected people.[24] However, neurological problems emerge in approximately 50% of HIV patients.[25] The neurocognitive damage often accelerates during the clinical treatment of the AIDS/HIV infection,[26] and remains even after suppression of the peripheral viral infection.[27] Neuronal injury during the antiretroviral therapy may arise from unknown mechanisms through toxins, pro-inflammatory cytokines, reactive oxygen species (ROS) and nitric oxide (NO) released by activated glial cells in response to residual viral replication.[28]

Activation of microglia, the brain's resident macrophages, has been extensively reported as one of the most important contributors of HIV-related neuroinflammation,[29] and in some case the antiretroviral therapy is able to revert this activation.[30] To verify whether IAS derivatives could interfere with the inflammatory status of microglia, BV2 cells were treated with lipopolysaccharide (LPS) (50 ng/mL), a pro-inflammatory stimulus that is elevated in the blood of HIV+ individuals,[31] in presence or absence of different doses of compound **23**, one of most potent HIV-1 NNRTI of the series, and the amount of NO released by the cells was measured, EFV was used as reference compound. Data showed that both **23** and EFV treatments were able to reduce LPS-induced NO release at 1 μM and 10 μM concentrations (Figure 2S, Supporting Information).

The pro-inflammatory or anti-inflammatory profile of BV2 cells treated with **23** or EFV was analyzed as expression of M1 (pro-inflammatory) and M2 (anti-inflammatory) mRNAs. Compounds **23**

and EFV differently decreased the expression of CD86 and iNOS M1 genes. As shown in Figure 4, both iNOS and CD86 were significantly reduced by **23**, while only iNOS was reduced by EFV treatment. These treatments did not alter the expression of the anti-inflammatory genes CD163 and Fizz.

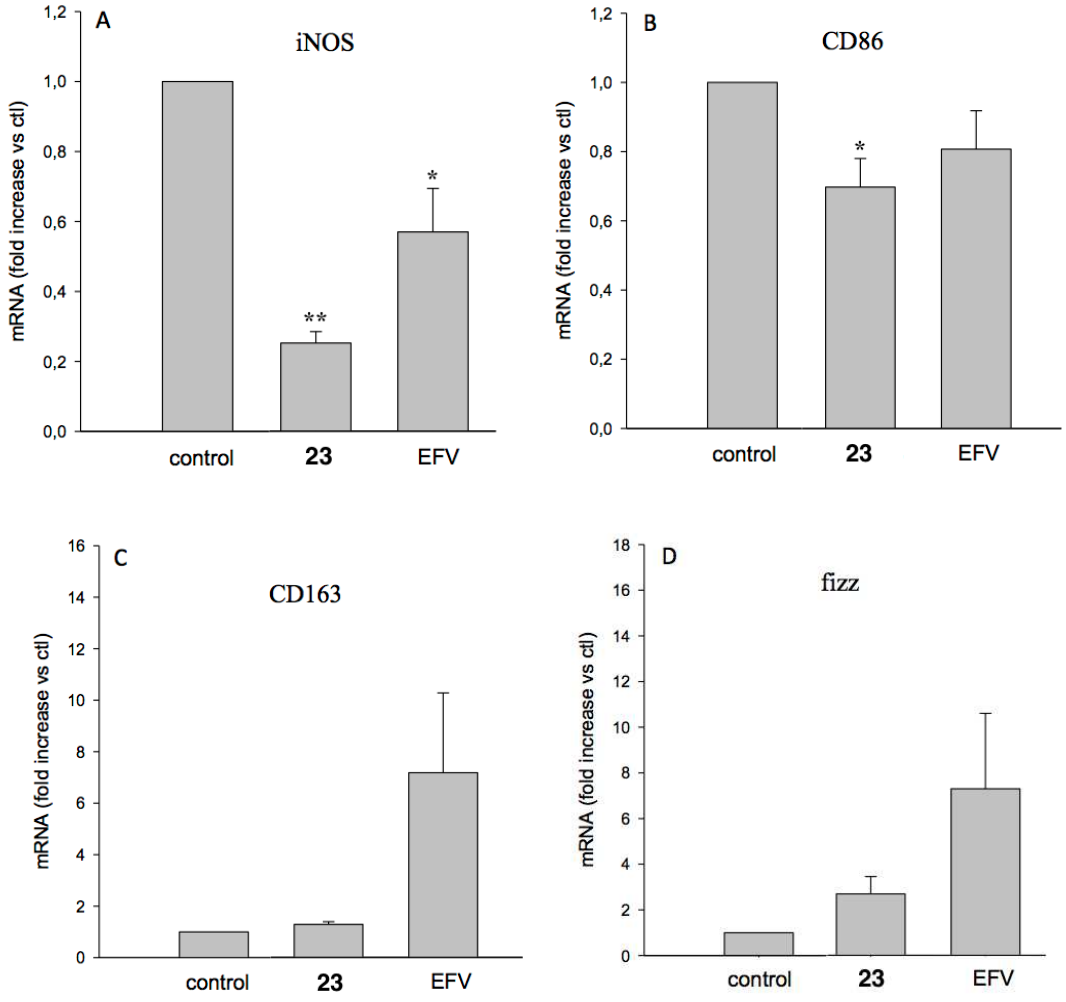

Figure 4. 23 reduced the pro inflammatory M1-related genes on BV2 cells. BV2 cells were treated with 10^3 nM (*R,S*)-**23** or EFV. mRNA expression of M1 (iNOS and CD86) and M2 (CD163 and FIZZ) related genes was assayed by RT-PCR. Data are expressed as fold increase vs ctl. N=4; *p<0,05 and **p<0,001 vs ctrl by Student's *t*-test.

To exclude the possibility that the effects could be due to a different rate of cell proliferation, BV2 microglial cells were cultured in presence of **23** or EFV at different doses (10 nM, 10^2 nM, 10^3 nM and 10^4 nM) and the proliferation rate of these cells was evaluated. Data show that the treatments did not alter the BV2 cell proliferation at any doses (Figure 3S, Supporting Information).

HIV-mediated microglia activation is responsible of release of neurotoxic factors such as excitatory molecules[32] and inflammatory cytokines,[33] resulting in neuronal dysfunction and cell death. To verify the effect on damaged neurons, compound **23** was administrated to hippocampal neuronal cultures in the presence of 100 μM glutamate as a neurotoxic stimulus. The compound proved to protect neurons from the excitotoxic insult. Notably, EFV was not efficacious to contrast the neurotoxic effect of glutamate (Figure 5).

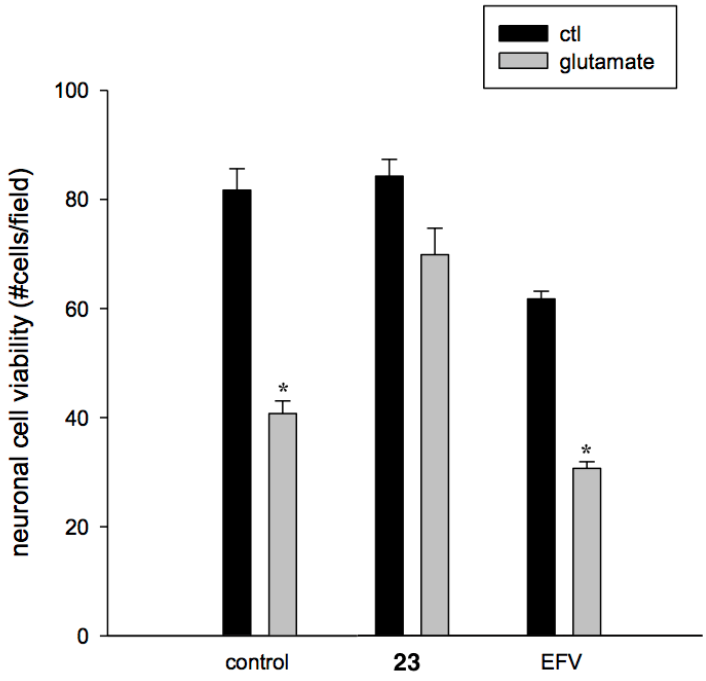

Figure 5. 23 treatment protect neurons against glutamate excitotoxicity. Neuronal cultures were stimulated with 100 μM glutamate in presence or absence of 10^3 nM **23** or EFV. Data are expressed as number of cell/optical field. N=3, *p<0,05 vs CTL by Kruskal-Wallis One Way Analysis of Variance (Dunn's method).

In Silico Prediction of Physicochemical Properties. The physicochemical properties of compounds **8**, **23** and **25** assessed by SwissADME[34] and QikProp[35] programs are shown in Table 7. The predicted physicochemical properties of derivatives **9-22**, **24** and **26-37** are reported in Table 1S, Supporting Information. Compounds **8**, **23** and **25** matched Lipinski's rule of five,[36] namely logP <5, H-bond donors ≤5, H-bond acceptors ≤10 and a molecular weight <500.[36] Derivative **8** did not show violation of Lipinski's rule of five (Rule of five = 4), while derivatives **23** and **25** showed one violation (molecular weight >500; Rule of five = 3). Compounds **8**, **23** and **25** exhibited significant values in the topological polar surface area (TPSA),[37] apparent Caco-2 and madin-carby canine kidney (MDCK) cells permeability predictions. These results show that compounds **8**, **23** and **25** have the potential to diffuse across membranes.

Table 7. In silico physicochemical properties of **8**, **23** and **25**.

Cmpd	LogP[a]	H-bond Acc.[b]	H-bond Don.[c]	MW[d]	TPSA[e]	QPP Caco[f]	QPP MDCK[g]
8	4.26	4	2	484.97	87.41	1595.51	3021.29
23	2.03	5	3	525.03	129.40	202.03	333.34
25	2.22	5	3	539.06	129.40	286.71	457.122

Physicochemical properties predicted by SwissADME:[34] [a]Octanol-water partition coefficient predictor by topological method implemented from Moriguchi;[38,39] [b]Number of H-bond acceptors; [c]Number of H-bond donors; [d]Molecular Weight; [e]Molecular polar surface area: this parameter correlates with human intestinal absorption (<140).[37] Physicochemical properties predicted by QikProp: [f]QPP Caco - Apparent Caco-2 permeability (nm/sec) (<25 poor, >500 great); [g]QPP MDCK - Apparent MDCK permeability (nm/sec) (<25 poor, >500 great).

CONCLUSION

We designed and synthesized new IAS derivatives **8-37** to explore the SARs at the nitrogen of the indole-2-carboxamide. The new IASs inhibited the HIV-1 WT NL4-3 strain in MT-4 cells with EC_{50} values at subnanomolar concentrations (except compounds **10** and **26**), and showed potent

inhibition of the mutant K103N, Y181C, Y188L and K103N-Y181C HIV-1 strains. Six racemic mixtures, **8**, **23-25**, **31** and **33**, were separated into their pure enantiomers. The (*R*)-enantiomers of IAS derivatives bearing the chiral type B unit (α-methylbenzyl) were superior to the (*S*)-counterparts (compare (*R*)-**8** with (*S*)-**8**, (*R*)-**3** with (*S*)-**3**,[21] and (*R*)-**5** with (*S*)-**5**[22]). On the contrary, in the case of IAS derivatives bearing the chiral type A unit (alanine) the (*S*)-enantiomer was more potent than the corresponding (*R*)-enantiomer (compare (*S*)-**23** with (*R*)-**23**), (*S*)-**31** with (*R*)-**31,** (*S*)-**33** and (*R*)-**33**). The IASs (*S,R*)-**25** and (*S,S*)-**25** bearing the chiral type A+B units ((*S*)-alanine and (*R*)- or (*S*)-(1-(pyridin-4-yl)ethyl moieties) were superior to the corresponding (*R,S*)-**25** and (*R,R*)-**25** counterparts. The docking results showed consistent binding modes in the HIV-1 WT RT as well as in the mutated K103N, Y181C and K103N-Y181C RTs. The biological results generally correlated with the length of the linker and the configuration of the asymmatric center: the *(R)* enantiomer of IASs bearing the short linker (chiral type B) and the *(S)* enantiomer with the longer linker (chiral type A unit) were superior to the corresponding counterparts. Compound **23** reduced the expression of both iNOS and CD86 (M1 genes) in BV2 cells while only iNOS was reduced by EFV treatment. On administration to hippocampal neuronal cultures in the presence of 100 μM glutamate as a neurotoxic stimulus, compound **23** protected neurons from the excitotoxic insult, while EFV did not contrast the neurotoxic effect of glutamate. The present results highlight the introduction of chiral unit(s), such us of (*S*)-alanine and (*R*)-(α-heterocyclylethyl), as a valuable strategy for the design of new series of IAS NNRTIs with improved resistance profile against the mutant HIV-1 strains and reduced neurotoxic effects. Based on these valuable information, the synthesis of new IAS derivatives is in progress in our laboratory and the results will be reported in due course.

EXPERIMENTAL SECTION

1. Chemistry. All reagents and solvents were handled according to material safety data sheet of the supplier and were used as purchased without further purification. Organic solutions were dried over anhydrous sodium sulfate. Evaporation of the solvents was carried out on a Büchi Rotavapor R-210 equipped with a Büchi V-850 vacuum controller and a Büchi V-700 vacuum pump. Column chromatography was performed on columns packed with silica gel from Macherey-Nagel (70−230 mesh). Silica gel thin layer chromatography (TLC) cards from Macherey-Nagel (silica gel precoated aluminum cards with fluorescent indicator visualizable at 254 nm) were used for TLC. Developed plates were visualized with a Spectroline ENF 260C/FE UV apparatus. Melting points (mp) were determined on a Stuart Scientific SMP1 apparatus and are uncorrected. Infrared spectra (IR) were recorded on a PerkinElmer Spectrum 100 FT-IR spectrophotometer equipped with universal attenuated total reflectance accessory and IR data acquired and processed by Spectrum 10.03.00.0069 software. Band position and absorption ranges are given in cm^{-1}. Proton nuclear magnetic resonance (^{1}H NMR) and carbon-13 nuclear magnetic resonance (^{13}C NMR) spectra were recorded with a Varian Mercury (300 MHz) or a Bruker Avance (400 MHz) spectrometer in the indicated solvent. Fid files were processed by MestreLab Research SL MestreReNova 6.2.1−769 software. Chemical shifts are expressed in δ units (ppm) from tetramethylsilane. Elemental analyses of biologically evaluated compounds were found to be within ±0.4% of the theoretical values and their purity was found to be >95% by high pressure liquid chromatography (HPLC). The HPLC system used (Dionex UltiMate 3000, Thermo Fisher Scientific Inc.) consisted of a SR-3000 solvent rack, a LPG-3400SD quaternary analytical pump, a TCC-3000SD column compartment, a DAD-3000 diode array detector, and an analytical manual injection valve with a 20 μL loop. Samples were dissolved in acetonitrile (1 mg/mL). HPLC analysis was performed by using an Acclaim 120 C18 column (5 □m, 4.6 mm × 250 mm, Thermo Fisher Scientific Inc.), at 25 ± 1 °C with an appropriate solvent gradient (acetonitrile/water),

flow rate of 1.0 mL/min and signal detector at 206, 230, 254 and 365 nm. Chromatographic data were acquired and processed by Chromeleon 6.80 SR15 Build 4656 software (Thermo Fisher Scientific Inc.).

General Procedure A: Derivatives 8-14 and 17-37. A mixture of acid (0.60 mmol) in anhydrous DMF (10 mL/mmol), amine (1.8 mmol), triethylamine (1.8 mmol) and PyBOP reagent (0.60 mmol) was stirred at 25 °C for 12 h. The reaction mixture was diluted with water and extracted with ethyl acetate. The organic layer was washed with brine, dried and filtered. Removal of the solvent gave a residue that was purified by column chromatography (silica gel, ethyl acetate:*n*-hexane = 1:2 as eluent).

General Procedure B: Derivatives 15 and 16. To a solution of acid (0.385 mmol) in anhydrous CH_2Cl_2 (15 mL/mmol), pyridine (0.155 mmol) and oxalyl chloride (0.424 mmol) were added at room temperature. The mixture was stirred for 2 h and then the amine (0.424 mmol) was added. The mixture was stirred overnight, then diluted with water and extracted with ethyl acetate. The organic layer was washed with brine, dried and filtered. Removal of the solvent gave a residue that was purified by column chromatography (silica gel, ethyl acetate:*n*-hexane = 1:2 as eluent).

General Procedure C: Derivative 17. 1,1′-Carbonyldiimidazole (0.29 mmol) was added to a suspension of acid (0.27 mmol) in anhydrous THF (20 mL/mmol). The reaction mixture was stirred at 25 °C for 2 h, then the amine (0.27 mmol) was added. The reaction mixture was stirred at 25 °C for 2 h and diluted with water and extracted with ethyl acetate. The organic layer was washed with brine, dried and filtered. Removal of the solvent gave a residue that was purified by column chromatography (silica gel, ethyl acetate:*n*-hexane = 3:2 as eluent) and then triturated in *n*-hexane:acetonitrile = 7:3.

*1.1. 5-Chloro-3-((3,5-dimethylphenyl)sulfonyl)-N-(1-(2-fluorophenyl)ethyl)-1H-indole-2-carboxamide (**8**).* Synthesized following general procedure A, starting from **38**[7] and 1-(2-fluorophenyl)ethanamine. Yield 78 %, mp 215-217 °C (from ethanol). ^{1}H NMR (400 MHz, DMSO-d_6): δ 1.53 (s, 3H), 2.27 (s, 6H), 5.38-5.46 (m, 1H), 7.19-7.25 (m, 3H), 7.32-7.34 (m, 2H), 7.51-7.56 (m, 4H), 7.95 (s, 1H), 9.47 (br s, 1H disappeared on treatment with D_2O), 13.03 ppm (br s, 1H, disappeared

on treatment with D_2O). ^{13}C NMR (300 MHz, DMSO-d_6): δ 21.17, 21.78, 44.04, 111.92, 115.37, 115.69, 115.98, 119.40, 123.98, 125.01, 125.06, 125.23, 125.78, 127.76, 128.18, 128.24, 129.47, 129.58, 130.49, 130.67, 133.37, 135.16, 137.18, 139.44, 143.01, 158.81 ppm. IR: ν 1651, 3252 cm^{-1}. Anal. ($C_{25}H_{22}ClFN_2O_3S$ (484,97)) C, H, N, Cl, F, S.

*1.2. 5-Chloro-3-((3,5-dimethylphenyl)sulfonyl)-N-(1-(furan-2-yl)ethyl)-1H-indole-2-carboxamide (**9**).* Synthesized following general procedure A, starting from **38**[7] and 1-(furan-2-yl)ethanamine. Yield 36%, mp 193-195 °C (from ethanol). ^1H NMR (400 MHz, DMSO-d_6): δ 1.54 (d, J = 7.0 Hz, 3H), 2.29 (s, 6H), 5.26-5.30 (m, 1H), 6.43-6.45 (m, 2H), 7.26 (s, 1H), 7.33 (dd, J = 2.2 and 8.8 Hz, 1H), 7.52-7.54 (m, 1H), 7.58 (s, 2H), 7.63-7.64 (m, 1H), 7.95 (d, J = 1.6 Hz, 1H)), 9.36 (d, J = 8.2 Hz, 1H, disappeared on treatment with D_2O), 13.03 ppm (br s, 1H, disappeared on treatment with D_2O). ^{13}C NMR (300 MHz, DMSO-d_6): δ 19.63, 21.21, 43.48, 106.40, 110.87, 112.01, 115.39, 119.41, 124.03, 125.23, 125.75, 127.76, 133.35, 135.19, 139.45, 142.74, 142.94, 155.38, 158.82 ppm. IR: ν 1650, 3235 cm^{-1}. Anal. ($C_{23}H_{21}ClN_2O_4S$ (456.94)) C, H, N, Cl, S.

*1.3. 5-Chloro-N-((4-chlorophenyl)(cyclopropyl)methyl)-3-((3,5-dimethylphenyl)sulfonyl)-1H-indole-2-carboxamide (**10**).* Synthesized following general procedure A, starting from **38**[7] and (4-chlorophenyl)(cyclopropyl)methanamine. Yield 54%, mp 243-245 °C (from ethanol). ^1H NMR (400 MHz, DMSO-d_6): δ 0.51-0.61 (m, 4H), 1.23-1.31 (m, 1H), 2.27 (s, 6H), 4.48-4.52 (m, 1H), 7.25 (s, 1H), 7.33 (dd, J = 2.1 and 8.9 Hz, 1H), 7.41-7.43 (m, 2H), 7.51-7.54 (m, 3H), 7.59 (s, 2H), 7.94 (d, J = 2.0 Hz, 1H), 9.60 (d, J = 7.0 Hz, 1H, disappeared on treatment with D_2O), 13.00 ppm (br s, 1H, disappeared on treatment with D_2O). ^{13}C NMR (300 MHz, DMSO-d_6): δ 4.14, 4.47, 17.39, 21.18, 57.38, 111.82, 115.41, 119.41, 123.97, 125.22, 125.86, 127.77, 128.68, 129.12, 132.11, 133.42, 135.18, 137.15, 139.46, 141.74, 143.00, 158.91 ppm. IR: ν 1647, 3180, 3288 cm^{-1}. Anal. ($C_{27}H_{24}Cl_2N_2O_3S$ (527.46)) C, H, N, Cl, S.

*1.4. 5-Chloro-3-((3,5-dimethylphenyl)sulfonyl)-N-(2-fluoro-6-methoxybenzyl)-1H-indole-2-carboxamide (**11**).* Synthesized following general procedure A, starting from **38**[7] and (2-fluoro-6-methoxyphenyl)methanamine. Yield 52%, mp 295-297 °C (from ethanol). ^{1}H NMR (400 MHz, DMSO-d_6): δ 2.23 (s, 6H), 3.85 (s, 3H), 4.61 (d, J = 4.9 Hz, 2H), 6.86 (t, J = 8.5 Hz, 1H), 6.94 (d, J = 7.9 Hz, 1H), 7.23 (s, 1H), 7.30-7.40 (m, 2H), 7.44 (s, 2H), 7.51 (d, J = 8.2 Hz, 1H), 7.99 (d, J = 2.0 Hz, 1H), 9.23 (br s, 1H, disappeared on treatment with D_2O), 13.06 ppm (br s, 1H, disappeared on treatment with D_2O). ^{13}C NMR (300 MHz, DMSO-d_6): δ 20.44, 47.40, 47.68, 47.96, 48.24, 48.52, 56.09, 107.21, 107.70, 108.04, 112.52, 115.18, 117.96, 119.97, 123.54, 125.53, 126.70, 126.94, 128.31, 130.25, 130.40, 133.32, 135.19, 139.78, 162.14 ppm. IR: v 1645, 3195 cm^{-1}. Anal. ($C_{25}H_{22}ClFN_2O_4S$ (500.97)) C, H, N, Cl, F, S.

*1.5. 5-Chloro-N-(1-(3,5-difluorophenyl)ethyl)-3-((3,5-dimethylphenyl)sulfonyl)-1H-indole-2-carboxamide (**12**).* Synthesized following general procedure A, starting from **38**[7] and 1-(3,5-difluorophenyl)ethanamine. Yield 73%, mp 238-240 °C (from ethanol). ^{1}H NMR (400 MHz, DMSO-d_6): δ 1.50 (d, J = 7.0 Hz, 3H), 2.28 (s, 6H), 5.19-5.22 (m, 1H), 7.10-7.14 (m, 1H), 7.21-7.24 (m, 3H), 7.34 (d, J = 2.1 and J = 8.8 Hz, 1H), 7.53-7.55 (m, 1H), 7.60 (s, 2H), 7.92 (d, J = 2.0 Hz, 1H), 9.42 (d, J = 7.3 Hz, 1H disappeared on treatment with D_2O), 13.04 ppm (br s, 1H, disappeared on treatment with D_2O). ^{13}C NMR (300 MHz, DMSO-d_6,): δ 22.17, 22.44, 49.03, 102.40, 102.74, 103.09, 109.75, 110.08, 111.95, 115.29, 119.29, 124.16, 125.08, 127.66, 133.41, 135.05, 137.83, 139.34, 143.03, 159.42, 161.17, 164.42 ppm. IR: v 1648, 2923, 3215 cm^{-1}. Anal. ($C_{25}H_{21}ClF_2N_2O_3S$ (502.96)) C, H, N, Cl, F, S.

*1.6. 5-Chloro-3-((3,5-dimethylphenyl)sulfonyl)-N-(2-fluoro-1-phenylethyl)-1H-indole-2-carboxamide (**13**).* Synthesized following general procedure A, starting from **38**[7] and 2-fluoro-1-phenylethanamine. Yield 52%, mp 216-218 °C (from ethanol). ^{1}H NMR (400 MHz, DMSO-d_6): δ 2.26 (s, 6H), 4.66-4.68 (m, 1H), 4.78-4.80 (m, 1H), 5.42-5.52 (m, 1H), 7.25 (s, 1H), 7.32-7.42 (m, 4H),

7.51-7.55 (m, 3H), 7.59 (s, 2H), 7.97 (d, *J* = 1.9 Hz, 1H), 9.74 (d, *J* = 7.9 Hz, 1H, disappeared on treatment with D_2O), 13.08 ppm (br d, *J* = 4.6 Hz, 1H, disappeared on treatment with D_2O). ^{13}C NMR (300 MHz, DMSO-d_6,): δ□21.14, 53.83, 54.09, 83.87, 86.17, 112.17, 115.46, 119.47, 123.99, 125.36, 125.83, 127.73, 127.85, 128.26, 128.96, 133.42, 135.22, 136.57, 137.80, 137.87, 139.50, 142.88, 159.36 ppm. IR: *v* 1650, 3235 cm^{-1}. Anal. ($C_{25}H_{22}ClFN_2O_3S$ (484.97)) C, H, N, Cl, F, S.

*1.7. 5-Chloro-N-(2,3-difluorobenzyl)-3-((3,5-dimethylphenyl)sulfonyl)-1H-indole-2-carboxamide (**14**).* Synthesized following general procedure A, starting from **38**[7] and (2,3-difluorophenyl)methanamine. Yield 47%, mp 255-257 °C (from ethanol). ^1H NMR (400 MHz, DMSO-d_6): δ 2.27 (s, 6H), 4.65 (d, *J* = 5.7 Hz, 2H), 7.20-7.24 (m, 2H), 7.32-7.41 (m, 3H), 7.52-7.54 (m, 1H), 7.59 (s, 2H), 7.93 (d, *J* = 1.9 Hz, 1H), 9.50 (t, *J* = 5.6 Hz, 1H, disappeared on treatment with D_2O) 13.07 ppm (br s, 1H, disappeared on treatment with D_2O). ^{13}C NMR (300 MHz, DMSO-d_6): δ□21.17, 37.06, 112.12, 115.35, 116.71, 116.93, 119.34, 124.10, 125.20, 125.61, 127.72, 127.99, 128.14, 133.40, 135.10, 137.19, 139.37, 142.93, 160.05 ppm. IR: *v* 1649, 3214 cm^{-1}. Anal. ($C_{24}H_{19}ClF_2N_2O_3S$ (488.93)) C, H, Cl, F, N, S.

*1.8. 5-Chloro-N-(4-cyanopyridin-2-yl)-3-((3,5-dimethylphenyl)sulfonyl)-1H-indole-2-carboxamide (**15**).* Synthesized following general procedure B, starting from **38**[7] and 2-aminoisonicotinonitrile. Yield 7%, mp 233-235 °C (from ethanol). ^1H NMR (400 MHz DMSO-d_6): δ 2,29 (s, 6H), 7.26 (s, 1H), 7.37 (dd, *J* = 2.0 and 8.5 Hz, 1H), 7.58-7.60 (m, 1H), 7.65 (s, 2H), 7.71 (dd, *J* = 1.4 e 5.1 Hz, 1H), 7.95 (d, *J* = 2.0 Hz, 1H), 8.49 (s, 1H), 8.69 (d, *J* = 5.1 Hz, 1H), 11.78 (br, s, 1H disappeared on treatment with D_2O), 13.28 ppm (br s, 1H, disappeared on treatment with D_2O). ^{13}C NMR (300 MHz, DMSO-d_6,): δ□21.18, 115.94, 116.20, 117.21, 117.89, 119.40, 121.80, 122.36, 124.29, 125.08, 125.11, 126.13, 127.66, 135.07, 139.36, 150.60, 152.16, 159.70 ppm. IR: *v* 1664, 2923, 3324 cm^{-1}. Anal. ($C_{23}H_{17}ClN_4O_3S$ (464.92)) C, H, N, Cl, S.

*1.9. 5-Chloro-N-(2-cyanopyridin-4-yl)-3-((3,5-dimethylphenyl)sulfonyl)-1H-indole-2-carboxamide (**16**).* Synthesized following general procedure B, starting from **38**[7] and 4-aminopicolinonitrile. Yield 11%,

mp 223-225 °C (from ethanol). ^{1}H NMR (400 MHz DMSO-*d*$_6$): δ 2.31-2.32 (m, 6H), 7.26-7.28 (m, 1H), 7.37 (dd, *J* = 2.7 and 8.9 Hz, 1H), 7.43 (dd, *J* = 2.1 e 8.8 Hz, 1H), 7.59-7.61 (m, 2H), 7.65 (s, 1H), 7.93-7.95 (m, 1H), 8.21 (d, *J* = 1,6 Hz, 1H), 8.72-8.73 (m, 1H), 11.68 (br, s, 1H disappeared on treatment with D_2O), 13.30 ppm (br s, 1H, disappeared on treatment with D_2O). ^{13}C NMR (300 MHz, DMSO-*d*$_6$): δ□21.21, 115.70, 117.21, 117.84, 118.74, 119.27, 120.38, 124.37, 124.46, 125.39, 127.86, 128.25, 131.14, 133.72, 134.14, 134.95, 135.11, 137.02, 139.08, 139.37, 142.77, 143.14, 146.46, 152.98, 159.47, 160.27 ppm. IR: *v* 1693, 2923, 3275 cm^{-1}. Anal. ($C_{23}H_{17}ClN_4O_3S$ (464.92)) C, H, Cl, N, S.

*1.10. N-(3-Aminobenzyl)-5-chloro-3-((3,5-dimethylphenyl)sulfonyl)-1H-indole-2-carboxamide (**17**).* Synthesized following general procedure C, starting from **38**[7] and 3-(aminomethyl)aniline. Yield 71%, mp 239-241 °C (from ethanol). ^{1}H NMR (400 MHz, DMSO-*d*$_6$): δ 2.27 (s, 6H), 4.42 (d, *J* = 5.8 Hz, 2H), 5.04 (s, 2H, disappeared on treatment with D_2O), 6.47-6.49 (m, 1H), 6.57-6.59 (m, 2H), 7.0 (t, *J* = 7.7 Hz, 1H), 7.24 (s, 1H), 7.33 (dd, *J* = 1.7 and 8.6 Hz, 1H), 7.52-7.54 (m, 1H), 7.58 (s, 2H), 7.95 (d, *J* = 2.0 Hz, 1H), 9.35 (t, *J* = 7.0 Hz, 1H, disappeared on treatment with D_2O), 13.04 ppm (br s, 1H, disappeared on treatment with D_2O). ^{13}C NMR (300 MHz, DMSO-*d*$_6$): δ□21.18, 43.79, 111.96, 113.32, 113.63, 115.40, 115.53, 119.45, 124.06, 125.21, 125.87, 127.74, 129.40, 133.32, 135.18, 137.11, 139.01, 139.47, 142.92, 149.18, 159.41 ppm. IR: *v* 1655, 2936, 3297 cm^{-1}. Anal. ($C_{24}H_{22}ClN_3O_3S$ (467.97)) C, H, N, Cl, S.

*1.11. N-((2-Amino-1H-benzo[d]imidazol-5-yl)methyl)-5-chloro-3-((3,5-dimethylphenyl)sulfonyl)-1H-indole-2-carboxamide (**18**).* Synthesized following general procedure A, starting from **38**[7] and 5-(aminomethyl)-1*H*-benzo[d]imidazol-2-amine. Yield 51%, mp 245-248 °C (from ethanol). ^{1}H NMR (400 MHz, DMSO-*d*$_6$/D_2O): δ 2.20 (s, 6H), 4.56 (s, 2H), 6.96-6.98 (m, 1H), 7.09 (d, *J* = 7.8 Hz, 1H), 7.21-7.22 (m, 2H), 7.34 (dd, *J* = 2.1 and 8.6 Hz, 1H), 7.50-7.54 (m, 3H), 7.93 (d, *J* = 1.6 Hz, 1H). IR: *v* 1648, 3276, 3364 cm^{-1}. ^{13}C NMR (300 MHz, DMSO-*d*$_6$,): δ□21.10, 44.19, 111.64, 111.78, 111.91,

115.38, 119.45, 119.93, 123.99, 125.18, 125.90, 127.74, 129.51, 133.32, 135.14, 137.20, 139.44, 142.94, 155.70, 159.23 ppm. Anal. ($C_{25}H_{22}ClN_5O_3S$ (507.99)) C, H, N, Cl, S.

*1.12. N-((1H-Indazol-3-yl)methyl)-5-chloro-3-((3,5-dimethylphenyl)sulfonyl)-1H-indole-2-carboxamide (**19**).* Synthesized following general procedure A, starting from **38**[7] and (1*H*-indazol-3-yl)methanamine. Yield 35%, mp 248-250 °C (from ethanol). ^{1}H NMR (400 MHz, DMSO-d_6): δ 2.20 (s, 6H), 4.93 (d, J = 5.6 Hz, 2H), 7.10 (t, J = 7.1 Hz, 1H), 7.21 (s, 1H), 7.30-7.37 (m, 2H), 7.50-7.55 (m, 4H), 7.90-7.93 (m, 1H), 7.97 (d, J = 2.0 Hz, 1H), 9.51 (br s, 1H, disappeared on treatment with D_2O), 12.96 (s, 1H, disappeared on treatment with D_2O), 13.06 (br s, 1H, disappeared on treatment with D_2O). ^{13}C NMR (400 MHz, DMSO-d_6): δ 21.11, 36.77, 110.58, 111.09, 113.80, 119.43, 120.27, 120.47, 120.81, 121.51, 121.56, 124.05, 126.68, 134.72, 135.10, 141.54, 154.43, 163.58 ppm. IR: v 1646, 2924, 3195 cm^{-1}. Anal. ($C_{25}H_{21}ClN_4O_3S$ (492.98)). C, H, N, Cl, S.

*1.13. 5-Chloro-3-((3,5-dimethylphenyl)sulfonyl)-N-(2-oxo-2-((1-phenylethyl)amino)ethyl)-1H-indole-2-carboxamide (**20**).* Synthesized following general procedure A, starting from **39** and 1-phenylethanamine. Yield 27%, mp 227-230 °C with decomposition (from ethanol). ^{1}H NMR (400 MHz, DMSO-d_6): δ 1.39 (d, J = 7.0 Hz, 3H), 2.27 (s, 6H), 4.07-4.10 (m, 2H), 4.97-5.02 (m, 1H), 7.21-7.34 (m, 7H), 7.54 (d, J = 8.6 Hz, 1H), 7.71 (s, 2H), 7.98 (s, 1H), 8.39 (d, J = 8.6 Hz, 1H, disappeared on treatment with D_2O), 9.41 (s, 1H, disappeared on treatment with D_2O), 13.08 ppm (br s, 1H, disappeared on treatment with D_2O). ^{13}C NMR (400 MHz, DMSO-d_6,): δ 21.12, 22.90, 43.35, 48.59, 112.02, 115.69, 119.46, 124.21, 125.29, 125.94, 126.42, 127.16, 127.78, 128.71, 135.29, 136.59, 139.56, 142.77, 144.82, 159.97, 167.45 ppm. IR: v 1535, 1648, 2921, 3258 cm^{-1}. Anal. ($C_{27}H_{26}ClN_3O_4S$ (524.03)): C, H, N, Cl, S.

*1.14. 5-Chloro-3-((3,5-dimethylphenyl)sulfonyl)-N-(1-oxo-1-((1-phenylethyl)amino)propan-2-yl)-1H-indole-2-carboxamide (**21**).* Synthesized following general procedure A, starting from **40** and 1-phenylethanamine. Yield 38%, mp 209-212 °C (from ethanol). ^{1}H NMR (400 MHz, DMSO-d_6): δ

1.36-1.43 (m, 6H), 2.22-2.30 (m, 6H), 4.61-4.66 (m, 1H), 4.95-5.01 (m, 1H), 7.21-7.37 (m, 7H), 7.52-7.57 (m, 1H), 7.69 (s, 2H), 8.00-8.02 (m, 1H), 8.49 (br s, 1H, disappeared on treatment with D_2O), 9.40 (br s, 1H, disappeared on treatment with D_2O), 13.06 ppm (br s, 1H, disappeared on treatment with D_2O). ^{13}C NMR (400 MHz, DMSO-*d*$_6$): δ 18.85, 19.02, 21.11, 21.16, 22.86, 22.98, 48.46, 48.59, 49.59, 49.70, 119.50, 124.08, 124.12, 126.23, 126.41, 127.11, 128.71, 128.74, 135.27, 139.53, 142.91, 144.70, 144.99, 170.85, 170.98 ppm. IR: *v* 1524, 1642, 3234 cm^{-1}. Anal. ($C_{28}H_{28}ClN_3O_4S$ (538.06)): C, H, N, Cl, S.

*1.15. 5-Chloro-3-((3,5-dimethylphenyl)sulfonyl)-N-(2-oxo-2-((pyridin-4-ylmethyl)amino)ethyl)-1H-indole-2-carboxamide (**22**).* Synthesized following general procedure A, starting from **39** and pyridin-4-ylmethanamine. Yield 45%, mp 276-279 °C (from ethanol). ^1H NMR (400 MHz, DMSO-*d*$_6$): δ 2.27 (s, 6H), 4.13 (d, *J* = 5.7, 2H), 4.39 (d, *J* = 6.0, 2H), 7.24 (s, 1H), 7.30-7.33 (m, 3H), 7.55 (d, *J* = 9.0 Hz, 1H), 7.70 (s, 2H), 7.97 (s, 1H), 8.47 (d, *J* = 4.9 Hz, 2H,), 8.64 (br s, 1H, disappeared on treatment with D_2O), 9.43 (s, 1H, disappeared on treatment with D_2O), 13.14 ppm (br s, 1H, disappeared on treatment with D_2O). ^{13}C NMR (400 MHz, DMSO-*d*$_6$): δ 21.16, 21.34, 41.59, 43.41, 111.83, 115.86, 119.34, 122.57, 124.27, 124.90, 126.14, 127.52, 135.05, 139.36, 143.09, 148.79, 149.85, 160.49, 169.01 ppm. IR: *v* 1558, 1647, 2922, 3310 cm^{-1}. Anal. ($C_{25}H_{23}ClN_4O_4S$ (510.99)): C, H, N, Cl, S.

*1.16. 5-Chloro-3-((3,5-dimethylphenyl)sulfonyl)-N-(1-oxo-1-((pyridin-4-ylmethyl)amino)propan-2-yl)-1H-indole-2-carboxamide (**23**).* Synthesized following general procedure A, starting from **40** and pyridin-4-ylmethanamine. Yield 49%, mp 112-115 °C (from ethanol). ^1H NMR (400 MHz, DMSO-*d*$_6$): δ 1.45 (d, *J* = 6.6 Hz, 3H), 2.28 (s, 6H), 4.38 (s, 2H), 4.61-4.65 (m, 1H), 7.26-7.29 (m, 3H), 7.35 (d, *J* = 8.1 Hz, 1H), 7.56 (d, *J* = 8.6 Hz, 1H), 7.68 (s, 2H), 8.00 (s, 1H), 8.48 (d, *J* = 4.4 Hz, 2H), 8.69 (t, *J* = 4.7 Hz, 1H, disappeared on treatment with D_2O) 9.43 (br s, 1H, disappeared on treatment with D_2O), 13.04 ppm (br s, 1H, disappeared on treatment with D_2O). ^{13}C NMR (300 MHz, DMSO-*d*$_6$,): δ 18.66, 21.11, 41.60, 49.83, 112.25, 115.56, 119.55, 121.84, 122.38, 124.09, 125.46, 125.92, 127.90, 133.33,

135.33, 136.10, 139.57, 142.71, 148.69, 149.93, 159.03, 172.22 ppm. IR: *v* 1566, 1648, 2936, 3220 cm^{-1}. Anal. ($C_{26}H_{25}ClN_4O_4S$ (525.02)): C, H, N, Cl, S.

*1.17. 5-Chloro-3-((3,5-dimethylphenyl)sulfonyl)-N-(2-oxo-2-((1-(pyridin-4-yl)ethyl)amino)ethyl)-1H-indole-2-carboxamide (**24**).* Synthesized following general procedure A, starting from **39** and 1-(pyridin-4-yl)ethanamine. Yield 40%, mp 238-240 °C dec. (from ethanol). ^{1}H NMR (400 MHz, DMSO-d_6): δ 1.39 (d, J = 6.5 Hz, 3H), 2.26 (s, 6H), 4.13 (d, J = 5.6 Hz, 2H), 4.96-4.99 (m, 1H), 7.25 (s, 1H), 7.35 (d, J = 4.8 Hz, 3H), 7.54 (d, J = 8.9 Hz, 1H), 7.71 (s, 2H), 7.97 (s, 1H), 8.48-8.49 (m, 2H), 8.52 (br s, 1H, disappeared on treatment with D_2O), 9.47 (t, J = 3.8 Hz, 1H, disappeared on treatment with D_2O), 13.10 ppm (br s, 1H, disappeared on treatment with D_2O). ^{13}C NMR (300 MHz, DMSO-d_6): δ 21.10, 22.11, 43.35, 47.94, 170.49, 119.50, 121.64, 124.19, 128.08, 135.44, 139.60, 142.71, 150.02, 153.60, 159.92, 162.21, 167.89, 171.85, 172.48, 174.76, 177.84, 181.21 ppm. IR: *v* 1561, 1648, 2926, 3258 cm^{-1}. Anal. ($C_{26}H_{25}ClN_4O_4S$ (525.02)) C, H, N, Cl, S.

*1.18. 5-Chloro-3-((3,5-dimethylphenyl)sulfonyl)-N-(1-oxo-1-((1-(pyridin-4-yl)ethyl)amino)propan-2-yl)-1H-indole-2-carboxamide (**25**).* Synthesized following general procedure A, starting from **40** and 1-(pyridin-4-yl)ethanamine. Yield 12%, mp 130-133 °C (from ethanol). ^{1}H NMR (400 MHz, DMSO-d_6): δ 1.38-1.43 (m, 6H), 2.23-2.28 (m, 6H), 4.60-4.66 (m, 1H), 4.91-4.98 (m, 1H), 7.23-7.26 (m, 1H), 7.33-7.35 (m, 3H), 7.54-7.56 (m, 1H), 7.67 (s, 2H), 7.99 (s, 1H), 8.45-8.50 (m, 2H), 8.55-8.62 (m, 1H, disappeared on treatment with D_2O), 9.39 (s, 1H, disappeared on treatment with D_2O), 13.08 ppm (br s, 1H, disappeared on treatment with D_2O). ^{13}C NMR (400 MHz, DMSO-d_6,): δ 18.74, 21.08, 21.14, 22.11, 47.96, 49.68, 108.92, 115.70, 119.48, 121.51, 121.61, 124.11, 127.82, 135.32, 139.56, 149.99, 150.05, 152.29, 153.02, 153.71, 154.51, 155.42, 159.02, 171.22 ppm. IR: *v* 1551, 1650, 2924, 3266 cm^{-1}. Anal. ($C_{27}H_{27}ClN_4O_4S$ (539.05)) C, H, N, Cl, S.

*1.19. 5-Chloro-3-((3,5-dimethylphenyl)sulfonyl)-N-(2-oxo-2-((2-(thiophen-2-yl)ethyl)amino)ethyl)-1H-indole-2-carboxamide (**26**).* Synthesized following general procedure A, starting from **39** and 2-

(thiophen-2-yl)ethanamine. Yield 42%, mp 160-164 °C (from ethanol). ^{1}H NMR (400 MHz, DMSO-*d*$_6$): δ 2.31 (s, 6H), 2.95-2.99 (m, 2H), 3.36-3.41 (m, 2H), 4.04 (d, *J* = 4.5 Hz, 2H), 6.90-6.95 (m, 2H), 7.27 (s, 1H), 7.31-7.37 (m, 2H), 7.55 (dd, *J* = 2.4 and 9.2 Hz, 1H), 7.73 (s, 2H), 8.00 (s, 1H), 8.19 (br s, 1H, disappeared on treatment with D_2O), 9.39 (br s, 1H, disappeared on treatment with D_2O), 13.07 ppm (br s, 1H, disappeared on treatment with D_2O). ^{13}C NMR (DMSO-*d*$_6$, 300 MHz): *δ* 21.18, 29.67, 41.53, 43.31, 109.98, 112.29, 115.56, 119.57, 124.20, 124.48, 125.46, 125.68, 127.44, 127.89, 133.37, 135.35, 139.58, 141.69, 142.71, 159.59, 164.08, 168.35 ppm. IR: *v* 1545, 1638, 2922, 3213 cm^{-1}. Anal. ($C_{25}H_{24}ClN_3O_4S_2$ (530.06)) C, H, N, Cl, S.

*1.20. 5-Chloro-3-((3,5-dimethylphenyl)sulfonyl)-N-(1-oxo-1-((2-(thiophen-2-yl)ethyl)amino) propan-2-yl)-1H-indole-2-carboxamide (**27**).* Synthesized following general procedure A, starting from **40** and 2-(thiophen-2-yl)ethanamine. Yield 41%, mp 227-230 °C (from ethanol). ^{1}H NMR (400 MHz, DMSO-*d*$_6$): *δ* 1.36 (d, *J* = 7.1 Hz, 3H), 2.30 (s, 6H), 2.95-2.99 (m, 2H), 3.36-3.45 (m, 2H), 4.51-4.58 (m, 1H), 6.89-6.91 (m, 1H), 6.93-6.95 (m, 1H), 7.27 (s, 1H), 7.32-7.37 (m, 2H), 7.56 (d, *J* = 8.6 Hz, 1H), 7.70 (s, 2H), 8.02 (s, 1H), 8.25 (t, *J* = 6.2 Hz, 1H, disappeared on treatment with D_2O), 9.37 (br s, 1H, disappeared on treatment with D_2O), 13.04 ppm (br s, 1H, disappeared on treatment with D_2O). ^{13}C NMR (300 MHz, DMSO-*d*$_6$): *δ* 18.86, 21.13, 29.60, 40.93, 49.70, 112.29, 115.52, 119.63, 124.10, 124.48, 125.51, 125.73, 125.97, 127.39, 127.94, 133.23, 135.38, 135.90, 139.60, 141.71, 142.73, 158.66, 171.74 ppm. IR: *v* 1566, 1648, 2936, 3217 cm^{-1}. Anal. ($C_{26}H_{26}ClN_3O_4S_2$ (544.09)) C, H, N, Cl, S.

*1.21. 5-Chloro-3-((3,5-dimethylphenyl)sulfonyl)-N-(2-((2-(2-methyl-5-nitro-1H-imidazol-1-yl)ethyl) amino)-2-oxoethyl)-1H-indole-2-carboxamide (**28**).* Synthesized following general procedure A, starting from **39** and 2-(2-methyl-5-nitro-1*H*-imidazol-1-yl)ethanamine. Yield 98%, mp 212-215 °C (from ethanol). ^{1}H NMR (300 MHz, DMSO-*d*$_6$): *δ* 2.30 (s, 6H), 2.42 (s, 3H), 3.48-3.55 (m, 2H), 3.97 (d, *J* = 5.7 Hz, 2H), 4.33-4.36 (m, 2H), 7.26 (s, 1H), 7.32-7.36 (m, 1H), 7.54 (d, *J* = 9.0 Hz, 1H), 7.70 (s,

2H), 7.99 (d, *J* = 9.8 Hz, 2H), 8.27 (t, *J* = 6.4 Hz, 1H, disappeared on treatment with D_2O), 9.37 (br s, 1H disappeared on treatment with D_2O), 13.84 ppm (br s, 1H, disappeared on treatment with D_2O). ^{13}C NMR (400 MHz, DMSO-d_6): δ 14.30, 21.15, 38.63, 43.07, 45.81, 115.71, 119.56, 121.01, 124.21, 125.40, 126.08, 127.82, 133.70, 135.33, 138.54, 138.92, 139.59, 140.54, 142.78, 151.93, 169.08 ppm. IR: *v* 1642, 1678, 2922, 3255 cm^{-1}. Anal. ($C_{25}H_{25}ClN_6O_6S$ (573.02)) C, H, N, Cl, S.

*1.22. 5-Chloro-3-((3,5-dimethylphenyl)sulfonyl)-N-(1-((2-(2-methyl-5-nitro-1H-imidazol-1 yl)ethyl)amino)-1-oxopropan-2-yl)-1H-indole-2-carboxamide (**29**).* Synthesized following general procedure A, starting from **40** and 2-(2-methyl-5-nitro-1*H*-imidazol-1-yl)ethanamine. Yield 74%, mp 138-140 °C with decomposition (from ethanol). ^1H NMR (300 MHz, DMSO-d_6): δ 1.25 (d, *J* = 7.0 Hz, 3H), 2.29 (s, 6H), 2.42 (s, 3H), 3.42-3.48 (m, 2H), 4.29-4.36 (m, 2H), 4.38-4.47 (m, 1H), 7.26 (s, 1H), 7.31-7.35 (m, 1H), 7.54 (d, *J* = 8.8 Hz, 1H), 7.66 (s, 2H), 7.98-8.00 (m, 2H), 8.32 (t, *J* = 6.1 Hz, 1H, disappeared on treatment with D_2O), 9.30 (br s, 1H, disappeared on treatment with D_2O), 13.00 ppm (br s, 1H, disappeared on treatment with D_2O). ^{13}C NMR (300 MHz, DMSO-d_6): δ 14.39, 18.42, 21.13, 38.38, 45.75, 49.51, 112.26, 115.54, 119.58, 124.06, 125.49, 125.95, 127.92, 133.28, 133.62, 135.35, 135.87, 138.99, 139.60, 142.70, 151.90, 158.73, 172.34 ppm. IR: *v* 1561, 1641, 2967, 3234 cm^{-1}. Anal. ($C_{26}H_{27}ClN_6O_6S$ (587.05)) C, H, N, Cl, S.

*1.23. 5-Chloro-3-((3,5-dimethylphenyl)sulfonyl)-N-(2-oxo-2-((pyrimidin-4-ylmethyl)amino)ethyl)-1H-indole-2-carboxamide (**30**).* Synthesized following general procedure A, from **39** and pyrimidin-4-ylmethanamine. Yield 67%, mp 233-235 °C (from ethanol). ^1H NMR (400 MHz, DMSO-d_6): δ 2.25 (s, 6H), 4.16 (d, *J* = 7.4 Hz, 2H), 4.43 (d, *J* = 7.8 Hz, 2H), 7.24 (s, 1H), 7.33 (dd, *J* = 2.1 and 11.5 Hz, 1H), 7.47 (d, *J* = 6.5 Hz, 1H), 7.54 (d, *J* = 11.6, 1H), 7.69 (s, 2H), 7.98 (d, *J* = 2.6 Hz, 1H), 8.69-8.72 (m, 2H), 9.09 (br s, 1H, disappeared on treatment with D_2O), 9.45 (t, *J* = 6.5 Hz, 1H, disappeared on treatment with D_2O), 13.05 ppm (br s, 1H, disappeared on treatment with D_2O). ^{13}C NMR (300 MHz, DMSO-d_6,): δ 21.08, 43.41, 44.11, 112.41, 115.53, 118.92, 119.58, 124.16, 125.48, 125.89, 127.92,

133.32, 135.30, 135.96, 139.55, 142.70, 157.71, 158.70, 159.76, 167.66, 169.05 ppm. IR: *v* 1555, 1649, 2928, 3265 cm^{-1}. Anal. ($C_{24}H_{22}ClN_5O_4S$ (511.98)) C, H, N, Cl, S.

*1.24. 5-Chloro-3-((3,5-dimethylphenyl)sulfonyl)-N-(1-oxo-1-((pyrimidin-4-ylmethyl)amino) propan-2-yl)-1H-indole-2-carboxamide (**31**).* Synthesized following general procedure A, starting from **40** and pyrimidin-4-ylmethanamine. Yield 80%, mp 108-110 °C (from ethanol). ^{1}H NMR (400 MHz, DMSO-*d*$_6$): δ 1.46 (d, *J* = 7.1 Hz, 3H), 2.26 (s, 6H), 4.42-4.44 (m, 2H), 4.64-4.67 (m, 1H), 7.25 (s, 1H), 7.36 (dd, *J* = 2.0 and 8.8 Hz, 1H), 7.46 (d, *J* = 5.0 Hz, 1H), 7.56 (d, *J* = 8.8 Hz, 1H), 7.68 (s, 2H), 8.0 (d, *J* = 2.0 Hz, 1H), 8.71 (d, *J* = 5.2 Hz, 1H), 8.81 (t, *J* = 6.0 Hz, 1H), 9.09 (d, *J* = 1.1 Hz, 1H, disappeared on treatment with D_2O), 9.46 (d, *J* = 6.7 Hz, 1H, disappeared on treatment with D_2O), 13.07 ppm (br s, 1H, disappeared on treatment with D_2O). ^{13}C NMR (300 MHz, DMSO-*d*$_6$,): δ 18.55, 21.08, 44.10, 49.84, 112.29, 115.54, 118.76, 119.55, 124.06, 125.47, 125.92, 127.91, 133.33, 135.32, 136.06, 139.56, 142.71, 157.75, 158.47, 159.07, 167.71, 172.48 ppm.

IR: *v* 1554, 1649, 2967, 3268 cm^{-1}. Anal. ($C_{25}H_{24}ClN_5O_4S$ (526.01)) C, H, N, Cl, S.

*1.25. 5-Chloro-3-((3,5-dimethylphenyl)sulfonyl)-N-(2-((furan-2-ylmethyl)amino)-2-oxoethyl)-1H-indole-2-carboxamide (**32**).* Synthesized following general procedure A, starting from **39** and furan-2-ylmethanamine. Yield 56%, mp 200-202 °C (from ethanol). ^{1}H NMR (300 MHz, DMSO-*d*$_6$): δ 2.27 (s, 6H), 4.05 (d, *J* = 5.4 Hz, 2H), 4.32 (d, *J* = 4.32 Hz, 2H), 6.25-6.26 (m, 1H), 6.35-6.36 (m, 1H), 7.23 (s, 1H), 7.30-7.33 (m, 1H), 7.51-7.54 (m, 2H), 7.69 (s, 2H), 7.97 (s, 1H), 8.48 (t, *J* = 5.3 Hz, 1H, disappeared on treatment with D_2O), 9.34 (br s, 1H, disappeared on treatment with D_2O), 13.02 ppm (br s, 1H, disappeared on treatment with D_2O). ^{13}C NMR (300 MHz, DMSO-*d*$_6$,): δ 21.10, 36.00, 43.22, 107.47, 110.90, 112.41, 115.52, 119.60, 124.20, 125.49, 125.88, 127.91, 133.26, 135.33, 135.90, 139.57, 142.64, 152.39, 159.55, 168.26 ppm. IR: *v* 1544, 1643, 2922, 3217 cm^{-1}. Anal. ($C_{24}H_{22}ClN_3O_5S$ (499.97)) C, H, N, Cl, S.

*1.26. 5-Chloro-3-((3,5-dimethylphenyl)sulfonyl)-N-(1-((furan-2-ylmethyl)amino)-1-oxopropan-2-yl)-1H-indole-2-carboxamide (**33**).* Synthesized following general procedure A, starting from **40** and furan-2-ylmethanamine. Yield 87%, mp 215-217 °C (from ethanol). ^{1}H NMR (300 MHz, DMSO-d_6): δ 1.38 (d, J = 5.3 Hz, 3H), 2.29 (s, 6H), 4.33-4.35 (m, 2H), 4.55-4.62 (m, 1H), 6.27 (d, J = 3.0 Hz, 1H), 6.38-6.39 (m, 1H), 7.26 (s, 1H), 7.32-7.35 (m, 1H), 7.54-7.57 (m, 2H), 7.68 (s, 2H), 8.01 (d, J = 1.9 Hz, 1H), 8.56 (t, J = 5.8 Hz, 1H, disappeared on treatment with D_2O), 9.36 (br s, 1H, disappeared on treatment with D_2O), 13.04 ppm (br s, 1H, disappeared on treatment with D_2O). ^{13}C NMR (DMSO-d_6, 300 MHz): δ 18.84, 21.12, 36.12, 49.63, 107.28, 110.91, 115.51, 119.61, 124.09, 125.50, 125.96, 127.93, 133.25, 135.35, 135.90, 139.59, 142.61, 142.72, 152.42, 158.71, 171.71 ppm. IR: v 1541, 1648, 3276 cm^{-1}. Anal. ($C_{25}H_{24}ClN_3O_5S$ (513.99)) C, H, N, Cl, S.

*1.27. 5-Chloro-3-((3,5-dimethylphenyl)sulfonyl)-N-(2-((2-fluorobenzyl)amino)-2-oxoethyl)-1H-indole-2-carboxamide (**34**).* Synthesized following general procedure A, starting from **39** and (2-fluorophenyl)methanamine. Yield 52%, mp 230-232 °C (from ethanol). ^{1}H NMR (300 MHz, DMSO-d_6): δ 2.27 (s, 6H), 4.10 (d, J = 5.3 Hz, 2H), 4.39 (d, J = 5.5 Hz, 2H), 7.11-7.18 (m, 2H), 7.24-7.41 (m, 4H), 7.52-7.55 (m, 1H), 7.69 (s, 2H), 7.98 (d, J = 1.6 Hz, 1H), 8.53 (t, J = 5.9 Hz, 1H, disappeared on treatment with D_2O), 9.40 (br s, 1H, disappeared on treatment with D_2O), 12.91 (br s, 1H, disappeared on treatment with D_2O). ^{13}C NMR (300 MHz, DMSO-d_6): δ 21.07, 36.47, 43.30, 112.40, 115.34, 115.58, 119.60, 124.18, 124.72, 125.46, 125.93, 126.24, 127.91, 129.47, 130.07, 133.35, 135.30, 136.01, 139.56, 142.73, 159.67, 168.52 ppm. IR: v 1542, 1632, 2920, 3216 cm^{-1}. Anal. ($C_{26}H_{23}ClFN_3O_4S$ (527,99)) C, H, N, Cl, F, S.

*1.28. 5-Chloro-3-((3,5-dimethylphenyl)sulfonyl)-N-(1-((2-fluorobenzyl)amino)-1-oxopropan-2-yl)-1H-indole-2-carboxamide (**35**).* Synthesized following general procedure A, starting from **40** and (2-fluorophenyl)methanamine. Yield 52%, mp 210-212 °C (from ethanol). ^{1}H NMR (400 MHz, DMSO-d_6): δ 1.41 (d, J = 7.0 Hz, 3H), 2.28 (s, 6H), 4.39 (d, J = 5.3 Hz, 2H), 4.60-4.63 (m, 1H), 7.13-719 (m,

2H), 7.25 (s, 1H), 7.27-7.39 (m, 3H), 7.54-7.56 (m, 1H), 7.68 (s, 2H), 8.01 (d, *J* = 1.8 Hz, 1H), 8.60 (t, *J* = 6.6 Hz, 1H, disappeared on treatment with D_2O), 9.37 (br s, 1H, disappeared on treatment with D_2O), 13.02 (br s, 1H, disappeared on treatment with D_2O). ^{13}C NMR (300 MHz, DMSO-d_6): δ 18.79, 21.09, 36.46, 49.72, 112.32, 115.35, 115.53, 119.61, 124.09, 124.77, 125.48, 125.96, 126.26, 127.92, 129.32, 129.43, 129.80, 133.29, 135.33, 135.96, 139.57, 142.72, 158.83, 171.95 ppm. IR: *v* 1568, 1647, 3275 cm^{-1}. Anal. ($C_{27}H_{25}ClFN_3O_4S$ (542,02)) C, H, N, Cl, F, S.

*1.29. 5-Chloro-3-((3,5-dimethylphenyl)sulfonyl)-N-(2-((1-(2-fluorophenyl)ethyl)amino)-2-oxoethyl)-1H-indole-2-carboxamide (**36**).* Synthesized following general procedure A, starting from **39** and 1-(2-fluorophenyl)ethanamine. Yield 29%, mp 230-232 °C (from ethanol). ^1H NMR (400 MHz, DMSO-d_6): δ 1.38 (d, *J* = 7.0 Hz, 3H), 2.26 (s, 6H), 4.10-4.11 (s, 2H), 5.21-5.24 (m, 1H), 7.12-7.16 (m, 2H), 7.25-7.28 (m, 2H), 7.34 (d, *J* = 9.2 Hz, 1H), 7.44 (t, *J* = 8.4 Hz, 1H), 7.54 (d, *J* = 8.6 Hz, 1H), 7.71 (s, 2H), 7.98 (s, 1H), 8.50 (d, *J* = 7.2 Hz, 1H, disappeared on treatment with D_2O), 9.42 (br s, 1H, disappeared on treatment with D_2O), 13.07 ppm (br s, 1H, disappeared on treatment with D_2O). ^{13}C NMR (400 MHz, DMSO-d_6,): δ 21.08, 21.90, 43.00, 43.25, 115.57, 115.71, 115.78, 119.47, 124.20, 124.88, 124.91, 125.29, 127.70, 127.75, 129.11, 129.19, 131.63, 131.77, 135.29, 139.56, 142.76, 158.63, 161.05, 167.58 ppm. IR: *v* 1538, 1637, 2925, 3219 cm^{-1}. Anal. ($C_{27}H_{25}ClFN_3O_4S$ (542.02)) C, H, N, Cl, F, S.

*1.30. 5-Chloro-3-((3,5-dimethylphenyl)sulfonyl)-N-(1-((1-(2-fluorophenyl)ethyl)amino)-1-oxopropan-2-yl)-1H-indole-2-carboxamide (**37**).* Synthesized following general procedure A, starting from **40** and 1-(2-fluorophenyl)ethanamine. Yield 70%, mp 200-202 °C (from ethanol). ^1H NMR (400 MHz, DMSO-d_6): δ 1.34-1.42 (m, 6H), 2.22-2.28 (m, 6H), 4.60-4.66 (m, 1H), 5.15-5.22 (m, 1H), 7.10-7.18 (m, 2H), 7.23-7.44 (m, 4H), 7.51-7.56 (m, 1H), 7.67-7.68 (m, 2H), 7.80 (s, 1H), 8.57 (d, *J* = 10.2 Hz, 1H, disappeared on treatment with D_2O), 9.36 (d, *J* = 12.4 Hz, 1H, disappeared on treatment with D_2O), 13.04 ppm (br s, 1H, disappeared on treatment with D_2O). ^{13}C NMR (300 MHz, DMSO-d_6,): δ 18.76,

18.96, 21.09, 21.83, 43.02, 49.54, 112.19, 115.51, 115.77, 119.56, 124.06, 124.87, 125.45, 125.91, 127.36, 127.63, 127.90, 129.03, 131.69, 131.86, 133.31, 135.32, 139.55, 142.67, 158.90, 161.47, 170.81 ppm. IR: *v* 1529, 1638, 2932, 3198 cm^{-1}. Anal. ($C_{28}H_{27}ClFN_3O_4S$ (556.05)) C, H, N, Cl, F, S.

2. Enantiomers

2.1. Enantioselective separations. Enantioselective HPLC analysis were performed by using stainless-steel Chiralpak IA (250 mm x 4.6 mm I.D. and 250 mm x 10 mm I.D.) and Chiralpak IC (250 mm x 4.6 mm I.D. and 250 mm x 10 mm I.D.) (Daicel, Chemical Industries, Tokyo, Japan) columns. HPLC-grade solvents were used as supplied by Aldrich (Milan, Italy). The HPLC apparatus consisted of a Perkin Elmer (Norwalk, CT, USA) 200 lc pump equipped with a Rheodyne (Cotati, CA, USA) injector, a 1000 μL sample loop, a HPLC Perkin Elmer oven and a Perkin Elmer 290 detector. The signal was acquired and processed by *Clarity* software.[40]

HPLC resolutions were carried out by using polysaccharide-based chiral stationary phases (CSPs). The CSP/eluent system and the corresponding chromatographic data for each compound analyzed are resumed as follows: **8**: Chiralpak IA/ethanol-DEA 100:0.2, k_1 = 0.67 (*R*), k_2 = 1.03 (*S*), temp.: 40 °C; **23**: Chiralpak IA/ethanol-DEA 100:0.2, k_1 = 0.33 (*R*), k_2 = 0.75 (*S*), temp.: 40 °C; **24**: Chiralpak IC/ethyl acetate-methanol-DEA 100:0.2, k_1 = 0.76 (*S*), k_2 = 1.51 (*R*), temp.: 25 °C; **25**: Chiralpak IC/*n*-hexane-ethanol-dichloromethane-DEA 40:15:45:0.3, k_1 = 0.58 (*R*,*S*), k_2 = 0.81 (*S*,*R*), k_3 = 1.20 (*S*,*S*), k_4 = 2.72 (*R*,*R*), temp.: 25 °C; **31**: Chiralpak IA/ethanol-dichloromethane-DEA 100:1:0.1, k_1 = 0.40 (*R*), k_2 = 1.05 (*S*), temp.: 40 °C; **33**: Chiralpak IA/n-hexane-ethyl acetate-DEA 50:50:0.1, k_1 = 1.94 (*S*), k_2 = 2.51 (*R*), temp.: 25 °C. k_1 and k_2 are the retention factors of the less retained enantiomer and the more retained enantiomer, respectively.

The CD spectra of (*S*)-**8** obtained by stereospecific synthesis and the enantiomers of **23** isolated at semipreparative scale were dissolved in ethanol (concentration about 0.2 mg/ml) in a quartz cell (0.1

cm-path length) at 25 °C and measured by using a Jasco[41] Model J-700 spectropolarimeter in the 400-200 nm spectral range. The spectra were average computed over three instrumental scans and the intensities were presented in terms of ellipticity values (mdeg).

2.2. Absolute configuration assignment. The absolute configurations of the enantiomers of **8, 23, 24, 31, 33** and four stereoisomers of **25** were empirically assigned by a combination of chemical correlation/enantioselective HPLC/circular dichroism methods. Commercially available (*S*)-enantiomers of the amines were used as starting material for the stereospecific synthesis of the *(S)*-IAS derivatives. The coupling reaction between the chiral amine and the corresponding carboxylic acid did not affect the stereogenic center and the designed enantiomer retained its absolute configuration during the conversion. The stereochemical course of the reactions was monitored by the HPLC conditions described in the experimental section.

The ee values ranged from 60 to 99% with the only exception of **2**3, for which a complete racemization was observed. The stereochemical assignment of the enantiomers of **23** was obtained by comparing their CD spectra with those of the enantiomers of **8** of known stereochemistry (Figure 4S, Supporting Information).

3. Molecular Modeling. All molecular modeling studies were performed on a MacPro dual 2.66 GHz Xeon running Ubuntu 12. The images in the manuscript were created with *PyMOL*.[42] The RTs structures were downloaded from the PDB website:[43] WT RT, 2RF2;[44] K103N RT, 3MED;[45] Y181C RT, 1UWB.[46] Hydrogen atoms were added to the protein using the Protonate #D option in *Molecular Operating Environment (MOE)* 2014.[47] Ligand structures were built with *MOE* and minimized using the MMFF94x force field until a rmsd gradient of 0.05 kcal/(mol·Å) was reached. The docking simulations were performed using *PLANTS*.[48] We set a binding lattice of 15 Å radius using all default settings used. Molecular dynamics was performed with the *Amber* 12 suite.[49] The minimized structure

was solvated in a periodic octahedron simulation box using TIP3P water molecules, providing a minimum of 10 Å of water between the protein surface and any periodic box edge. Ions were added to neutralize the charge of the total system. The water molecules and Cl^- ions were energy-minimized keeping the coordinates of the protein-ligand complex fixed (1000 cycle), and then the whole system was minimized (5000 cycle). Following minimization, the entire system was heated to 298 K (20 ps). The production (50 ns) simulation was conducted at 298 K with constant pressure and periodic boundary condition. Shake bond length condition was used (ntc = 2). Production was carried out on GeForce gtx780 gpu. Compounds were parametrized by Antechamber[50,51] using BCC charges. Trajectories analysis were carried out by cpptraj program.[52] Molecular dynamics snapshots were obtained by computing the average for the latest 3500 steps and then was selected as representative step the one with the lowest RMSD versus computed average. Binding free energy were computed by sietraj.[53,54]

4. Biological Assays

4.1. Inhibition of HIV-induced cytopathicity. Biological activity of the compounds was tested in the lymphoid MT-4 cell line (received from the NIH AIDS Reagent Program) against the WT HIV-1 NL4-3 strain and the different mutant HIV-1 strains, as described before.[55] Briefly, MT-4 cells were infected with the appropriate HIV-1 strain (or mock-infected to determine cytotoxicity) in the presence of different drug concentrations. At day five post-infection, a tetrazolium-based colorimetric method (MTT method) was used to evaluate the number of viable cells.

4.2. Enzymatic assay procedures. Chemicals. [^{3}H]dTTP (40 Ci/mmol) was from Perkinelmer and unlabelled dNTP's from Promega. Perkinelmer was the supplier of the GF/C filters. All other reagents were of analytical grade and purchased from Sigma. *Nucleic acid substrate*. The homopolymer poly(rA) (Pharmacia) was mixed at weight ratios in nucleotides of 10:1, to the oligomer oligo(dT)$_{12-18}$

(Pharmacia) in 20 mM Tris-HCl (pH 8.0), containing 20 mM KCl and 1 mM EDTA, heated at 65 °C for 5 min and then slowly cooled at room temperature. *Enzymatic assay.* The coexpression vectors pUC12N/p66(His)/p51with the wild-type or the mutant forms of HIV-1 RT p66 were kindly provided by Dr. S. H. Hughes (NCI-Frederick Cancer Research and Development Center). Proteins were expressed in *E. coli* and purified as described.[56] RNA-dependent DNA polymerase activity was assayed as follows: a final volume of 15 µL contained reaction buffer (50 mM Tris-HCl pH 7.5, 1 mM DTT, 0.2 mg/mL BSA, 4% glycerol), 10% DMSO, 10 mM $MgCl_2$, 0.5 µg of poly(rA)/oligo$(dT)_{10:1}$ (0.3 µM 3'-OH ends), 10 µM [3H]-dTTP (1Ci/mmol) and 2-4 nM RT. Reactions were incubated at 37 °C for the indicated time. 10 µL-Aliquots were then spotted on glass fiber filters GF/C which were immediately immersed in 5% ice-cold TCA. Filters were washed twice in 5% ice-cold TCA and once in ethanol for 5 min, dried and acid-precipitable radioactivity was quantitated by scintillation counting. Reactions were performed under the conditions described for the HIV-1 RT RNA-dependent DNA polymerase activity assay. Incorporation of radioactive dTTP into poly(rA)/oligo(dT) at different substrate (nucleic acid or dTTP) concentrations was monitored in the presence of increasing fixed inhibitor dose was monitored, and data were then plotted according to equation 1 using Graphpad Prism 5.0 software

$$ID_{50} = V = v/(1+([I]/ID_{50}))$$

Equation 1. V: maximum velocity of the reaction; v: reaction velocity; [I]: inhibitor concentration; ID_{50}: calculated inhibitor dose that conferred 50% enzymatic activity.

4.3. Cell line and neuronal cultures. BV2 cells were maintained in culture in DMEM containing 10% FBS. Cells were used up to passage 40. Primary hippocampal neuronal cultures were prepared from 0-2-day old (p0–p2) C57BL/6 mice. Briefly, after careful dissection from diencephalic structures, the meninges were removed and hippocampal tissues chopped and digested for 20 min at 37 °C in 0.025% trypsin and Hank's balanced salt solution (HBSS). Cells were washed twice with HBSS to

remove the excess of trypsin, mechanically dissociated in minimal essential medium (MEM) with Earl's Salts and GLUTAMAX supplemented with 10% dialyzed and heat inactivated FBS. Cells were plated at a density of 2 x 10^5 in the same medium on poly-L-lysine (100 μg/mL)-coated plastic 24-well dishes. After 2 h, the medium was replaced with serum- free Neurobasal/B27. Cells were kept at 37 °C in 5% CO_2 for 11 days. By this method we obtained 60-70% neurons, 30-35% astrocytes, 4-8% microglia, as previously reported.[57] Procedures were approved by the Italian Ministry of Health in accordance with the guidelines on the ethical use of animals from the European Community Council Directive of 22 September 2010 (2010/63/EU)

4.4. Nitrite assay. NO production of BV2 cells was assessed by measuring nitrite accumulation in the culture medium by Griess Reagent Kit according to manifacturer instructions (Molecular Probes, MA, USA). The absorbance was measured at 570 nm in a spectrophotometric microplate reader (BioTek Instruments Inc, VT, USA).

4.5. MTT cell viability assay. BV2 cell lines were seeded into multi-well plates and treated with vehicle or 10, 10^2, 10^3 or 10^4 nM (*R,S*)-**23** or EFV for 0-24-48 h. MTT (500 μg/mL) was added into each well for 2 h. DMSO was then added to stop the reaction and the produced formazan was measured at 570 nm in a spectrophotometric microplate reader (BioTek Instruments Inc, VT, USA). Viability of cells was expressed as % relative to 0 h.

4.6. Excitotoxicity assay. Hippocampal cultures were treated with 100 μM glutamate in Locke's buffer containing NaCl (154 mM), KCl (5.6 mM), $NaHCO_3$ (3.6 mM), HEPES (5 mM), $CaCl_2$ (2.3 mM), glucose (5.6 mM), glycine (10 mM) at pH 7.4 for 30 min in the presence or absence of (*R,S*)-**23** or EFV and then re-incubated in the conditioned culture medium for 18 h in the presence or absence of (*R,S*)-**23** or EFV. To evaluate neuron viability, hippocampal neuronal cultures were treated with detergent-containing buffer (0.05% ethyl hexadecyl dimethylammonium bromide, 0.028% acetic acid,

0.05% Triton X-100, 0.3 mM NaCl, 0.2 mM $MgCl_2$ in PBS pH 7.4) and viable nuclei counted in a hemacytometer as described.[58,59]

4.7. Real Time PCR. BV2 cells were treated with (*R,S*)-**23** or EFV. After 24 h total RNA was extracted with Trizol reagent (Invitrogen, Italy), quantified and retro-transcripted using IScriptTM Reverse Transcription Supermix (Biorad, Italy). Real Time PCR (RT-PCR) was carried out in an I-Cycler IQ Multicolor RT-PCR Detection System (Biorad, Italy) using SsoFast Eva Green Supermix (Biorad, Italy). The PCR protocol consisted of 40 cycles of denaturation at 95 °C for 30 s and annealing/extension at 58 °C for 30 s. The Ct values from each gene were normalized to the Ct value of GAPDH. Relative quantification was performed using the $2^{-\Delta\Delta Ct}$ method and expressed as fold increase. Primer sequences are: *gapdh*: fw TCGTCCCGTAGACAAAATGG, rev TTGAGGTCAATGAAGGGGTC; *inos:* fw, CATCGACCCGTCCACAGTAT, rev CAGAGGGGTAGGCTTGTCTC; *cd86*: fw, AGAACTTACGGAAGCACCCA, rev GGCAGATATGCAGTCCCATT; *cd163*: fw, TCTGGCTTGACAGCGTTTC, rev, TGTGTTTGTTGCCTGGATT; *fizz1*: fw, CCAATCCAGCTAACTATCCCTCC, rev, ACCCAGTAGCAGTCATCCCA.

ASSOCIATED CONTENT

Supporting Information

Additional chemical and biological material, including molecular formula strings, is available free of charge via the internet at http//pubs.acs.org.

AUTHOR INFORMATION

Corresponding Authors

*Phone: +39 06 4991 3404. Fax: +39 06 4991 39933. E-mail: giuseppe.laregina@uniroma1.it.

Notes

The authors declare no competing financial interest.

Funding Sources

This research was supported by grant year 2012 by Institut Pasteur Italy - Fondazione Cenci Bolognetti, Progetti per Avvio alla Ricerca from Sapienza University (V.F.), and and by project BFU2015-63800R from the Spanish MINECO (JAE).

Abbreviations

HIV-1, human immunodeficiency virus type; 1 AIDS, acquired immunodeficiency syndrome; NRTI, nucleoside reverse transcriptase inhibitor; NNRTI, non nucleoside reverse transcriptase inhibitor; ART, antiretroviral therapy; IAS, indolylarylsulfone; EFV, efavirenz; NVP, nevirapine; AZT, azidothymidine; ETR, etravirine; WT, wild type; SAR, structure-affinity relationship; PyBOP, benzotriazol-1-yl-oxytripyrrolidinophosphonium hexafluorophosphate; CSP, chiral stationary phase.

REFERENCES

(1) Global AIDS Update. 31 May 2016. UNAIDS 2016, Geneva, Switzerland. (accessed July 4, 2016).

(2) WHO. Consolidated guidelines on the use of antiretroviral drugs for treating and preventing HIV infection. 2nd ed. 2016. Publication date: June 9, 2016, , Geneva, Switzerland. (accessed July 4, 2016).

(3) Este, J. A.; Cihlar, T. Current status and challenges of antiretroviral research and therapy. *Antiviral Res.* **2010**, *8*5, 25-33.

(4) Cortez, K. J.; Maldarelli, F. Clinical management of HIV drug resistance. *Viruses* **2011**, *3*, 347-378.

(5) Hawkins, T. Understanding and managing the adverse effects of antiretroviral therapy. *Antiviral Res.* **2010**, *85*, 201-209.

(6) De Clercq, E. The nucleoside reverse transcriptase inhibitors, nonnucleoside reverse transcriptase inhibitors, and protease inhibitors in the treatment of HIV infections (AIDS). *Adv. Pharmacol.* **2013***, 67*, 317-358.

(7) Silvestri, R.; De Martino, G.; La Regina, G.; Artico, M.; Massa, S.; Vargiu, L.; Mura, M.; Loi, A. G.; Marceddu, T.; La Colla, P. Novel indolyl aryl sulfones active against HIV-1 carrying NNRTI resistance mutations: synthesis and SAR studies. *J. Med. Chem.* **2003**, *46*, 2482-2493.

(8) Silvestri, R.; Artico, M.; De Martino, G.; La Regina, G.; Loddo, R.; La Colla, M.; La Colla, P. Simple, short peptide derivatives of a sulfonylindolecarboxamide (L-737,126) active in vitro against HIV-1 wild-type and variants carrying non-nucleoside reverse transcriptase inhibitor resistance mutations. *J. Med. Chem.* **2004**, *47*, 3892-3896.

(9) Piscitelli, F.; Coluccia, A.; Brancale, A.; La Regina, G.; Sansone, A.; Giordano, C.; Balzarini, J.; Maga, G.; Zanoli, S.; Samuele, A.; Cirilli, R.; La Torre, F.; Lavecchia, A.; Novellino, E.; Silvestri, R. Indolylarylsulfones bearing natural and unnatural amino acids. Discovery of potent inhibitors of HIV-1 non-nucleoside wild type and resistant mutant strains reverse transcriptase and Coxsackie B4 virus. *J. Med. Chem.* **2009**, *52*, 1922-1934.

(10) Ragno, R.; Artico, M.; De Martino, G.; La Regina, G.; Coluccia, A.; Di Pasquali, A.; Silvestri, R. Docking and 3-D QSAR studies on indolyl aryl sulfones (IASs). Binding mode exploration at the HIV-1 reverse transcriptase nonnucleoside binding site and design of highly active *N*-(2-hydroxyethyl)carboxyamide and *N*-(2-hydroxyethyl)-carboxyhydrazide derivatives. *J. Med. Chem.* **2005**, *48*, 213-223.

(11) Ragno, R.; Coluccia, A.; La Regina, G.; De Martino, G.; Piscitelli, F.; Lavecchia, A.; Novellino, E.; Bergamini, A.; Ciaprini, C.; Sinistro, A.; Maga, G.; Crespan, E.; Artico, M.; Silvestri, R. Design, molecular modeling, synthesis and anti-HIV-1 activity of new indolyl aryl sulfones. Novel derivatives of the indole-2-carboxamide. *J. Med. Chem.* **2006**, *49*, 3172-3184.

(12) Guillemont, J.; Pasquier, E.; Palandjian, P.; Vernier, D.; Gaurrand, S.; Lewi, P. J.; Heeres, J.; de Jonge, M. R.; Koymans, L. M.; Daeyaert, F. F.; Vinkers, M. H.; Arnold, E.; Das, K.; Pauwels, R.; Andries, K.; de Béthune, M. P.; Bettens, E.; Hertogs, K.; Wigerinck, P.; Timmerman, P.; Janssen, P. A. Synthesis of novel diarylpyrimidine analogues and their antiviral activity against human immunodeficiency virus type 1. *J. Med. Chem.* **2005**, *48*, 2072-2079.

(13) La Regina, G.; Coluccia, A.; Silvestri, R. Looking for an active conformation of the future HIV-1 non-nucleoside reverse transcriptase inhibitors. *Antiviral Chem. Chemoth.* **2010**, *20*, 231-237.

(14) Chong, P.; Sebahar, P.; Youngman, M.; Garrido, D.; Zhang, H.; Stewart, E. L.; Nolte, R. T.; Wang, L.; Ferris, R. G.; Edelstein, M.; Weaver, K.; Mathis, A.; Peat, A. Rational design of potent non nucleoside inhibitors of HIV-1 reverse transcriptase. *J. Med. Chem.* **2012**, *55*, 10601-10609.

(15) La Regina, G.; Coluccia, A.; Brancale, A.; Piscitelli, F.; Gatti, V.; Maga, G.; Samuele, A.; Pannecouque, C.; Schols, D.; Balzarini, J.; Novellino, E.; Silvestri, R. Indolylarylsulfones as HIV-1 non-nucleoside reverse transcriptase inhibitors. New cyclic substituents at the indole- 2-carboxamide. *J. Med. Chem.* **2011**, *54*, 1587-1598.

(16) La Regina, G.; Coluccia, A.; Brancale, A.; Piscitelli, F.; Famiglini, V.; Cosconati, S.; Maga, G.; Samuele, A.; Gonzalez, E.; Clotet, B.; Schols, D.; Esté, J. A.; Novellino, E.; Silvestri, R. New nitrogen containing substituents at the indole-2-carboxamide yield high potent and broad

spectrum indolylarylsulfone HIV-1 non-nucleoside reverse transcriptase inhibitors. *J. Med. Chem.* **2012**, *55*, 6634-6638.

(17) Kang, D.; Fang, Z.; Li, Z.; Huang, B.; Zhang, H.; Lu, X.; Xu, H.; Zhou, Z.; Ding, X.; Daelemans, D.; De Clercq, E.; Pannecouque, E.; Zhan, P.; Liu, X. Design, synthesis, and evaluation of thiophene[3,2-*d*]pyrimidine derivatives as HIV-1 non-nucleoside reverse transcriptase inhibitors with significantly improved drug resistance profiles. *J. Med. Chem.* **2016**, *59*, 7991–8007.

(18) Zhan, P.; Pannecouque, C.; De Clercq, E.; Liu, X. Anti-HIV drug discovery and development: current innovations and future trends. *J. Med. Chem.* **2016**, *59*, 2849-2878.

(19) Menéndez-Arias, L.; Sebastián-Martín, A.; Álvarez, M. Viral reverse transcriptases. *Virus Res.* [Online early access]. DOI: 10.1016/j.virusres.2016.12.019. Published Online: Dec 30, 2016. http://www.sciencedirect.com.

(20) Famiglini, V.; Silvestri, R. Focus on chirality of HIV-1 non-nucleoside reverse transcriptase inhibitors. *Molecule*s **2016**, *21*, 221-240.

(21) Famiglini, V.; La Regina, G.; Coluccia, A.; Pelliccia, S.; Brancale, A.; Maga, G.; Crespan, E.; Badia, R.; Clotet, B.; Esté, J. A.; Cirilli, R.; Novellino, E.; Silvestri, R. New indolylarylsulfones as highly potent and broad spectrum HIV-1 non-nucleoside reverse transcriptase inhibitors. *Eur. J. Med. Chem.* **2014**, *80*, 101-111.

(22) Famiglini, V.; La Regina, G.; Coluccia, A.; Pelliccia, S.; Brancale, A.; Maga, G.; Crespan, E.; Badia, R.; Riveira-Muñoz, E.; Esté, J. A.; Ferretti, R.; Cirilli, R.; Zamperini, C.; Botta, M.; Schols, D.; Limongelli, V.; Agostino, B.; Novellino, E.; Silvestri, R. Indolylarylsulfones carrying a heterocyclic tail as very potent and broad spectrum HIV-1 non-nucleoside reverse transcriptase inhibitors. *J. Med. Chem.* **2014**, *57*, 9945-9957.

(23) Massarotti, A.; Coluccia, A. An in-silico approach aimed to clarify the role of Y181C and K103N HIV-1 reverse transcriptase mutations versus Indole Aryl Sulphones. *J. Mol. Graph. Model*. **2016**, *63*, 49-56.

(24) May, M. T.; Ingle, S. M. Life expectancy of HIV-positive adults: a review. *Sex. Health* **2011**, *8*, 526-533.

(25) Clifford, D. B. HIV-associated neurocognitive disease continues in the antiretroviral era. *Top HIV Med.* **2011**, *16*, 94-98.

(26) Grovit-Ferbas, K.; Harris-White, M. E. Thinking about HIV: the intersection of virus, neuroinflammation and cognitive dysfunction. *Immunol. Res.* **2010**, *48*, 40-58.

(27) Joska, J. A.; Gouse, H.; Paul, R. H.; Stein, D. J.; Flisher, A. J.. Does highly active antiretroviral therapy improve neurocognitive function? A systematic review. *J. Neurovir.* **2010**, *16*, 101-114.

(28) Lisi, L.; Tramutola, A.; Navarra, P.; Dello Russo, C. Antiretroviral agents increase NO production in gp120/IFNγ-stimulated cultures of rat microglia via an arginase-dependent mechanism. *J. Neuroimmunol.* **2014**, *266*, 24-32.

(29) (a) Nottet, H. S. Interactions between macrophages and brain microvascular endothelial cells: role in pathogenesis of HIV-1 infection and blood - brain barrier function. *J. Neurovir.* **1999**, *5*, 659-669; (b) Fischer-Smith, T.; Croul, S.; Adeniyi, A.; Rybicka, K.; Morgello, S.; Khalili, K.; Rappaport J. Macrophage/microglial accumulation and proliferating cell nuclear antigen expression in the central nervous system in human immunodeficiency virus encephalopathy. *Am. J. Pathol.* **2004,** *164*, 2089-2099; (c) Boven, L. A.; Middel, J.; Verhoef, J.; De Groot, C. J.; Nottet, H. S. Monocyte infiltration is highly associated with loss of the tight junction protein zonula occludens in HIV-1-associated dementia. *Neuropath. Appl. Neurobiol.* **2000**, *26*, 356-360.

(30) Anthony, I. C.; Ramage, S. N., Carnie, F. W.; Simmonds, P.; Bell, J. E. Influence of HAART on HIV-related CNS disease and neuroinflammation. *J. Neuropath. Exp. Neurol.* **2005**, *64*, 529-536.

(31) Brenchley, J. M.; Price, D. A.; Schacker, T. W.; Asher, T. E.; Silvestri, G.; Rao, S.; Kazzaz, Z.; Bornstein, E.; Lambotte, O.; Altmann, D.; Blazar, B. R.; Rodriguez. B.; Teixeira-Johnson, L.; Landay, A.; Martin, J. N.; Hecht, F. M.; Picker, L. J.; Lederman, M. M.; Deeks, S. G.; Douek, D. C. Microbial translocation is a cause of systemic immune activation in chronic HIV infection. *Nat. Med.* **2006**, *12*, 1365-1371.

(32) Huang, Y.; Zhao, L.; Jia, B.; Wu, L.; Li, Y.; Curthoys, N.; Zheng, J. C. Glutaminase dysregulation in HIV-1-infected human microglia mediates neurotoxicity: relevant to HIV-1-associated neurocognitive disorders. *J. Neurosci.* **2011**, *31*, 15195-15204; (b) Guillemin, G. J.; Kerr, S. J, Brew, B. J. Involvement of quinolinic acid in AIDS dementia complex. *Neurotox. Res.* **2005**, *7*, 103-123.

(33) Brabers, N. A.; Nottet, H. S. Role of the pro-inflammatory cytokines TNF-alpha and IL-1beta in HIV-associated dementia. *Eur. J. Clin. Invest.* **2006**, *36*, 447-458; (b) Walsh, J. G.; Reinke, S. N.; Mamik, M. K.; McKenzie, B. A.; Maingat, F.; Branton, W. G.; Broadhurst, D. I.; Power, C. Rapid inflammasome activation in microglia contributes to brain disease in HIV/AIDS. *Retrovirology* **2014**, *11*, 35; (c) Wesselingh, S. L.; Takahashi, K.; Glass, J. D.; McArthur, J. C.; Griffin, J. W, Griffin D. E. Cellular localization of tumor necrosis factor mRNA in neurological tissue from HIV-infected patients by combined reverse transcriptase/polymerase chain reaction in situ hybridization and immunohistochemistry. *J. Neuroimmunol.* **1997**, *74*, 1-8.

(34) SwissADME website for computation of physicochemical descriptors and ADME parameterrs prediction, Swiss Institute of Bioinformatics (SIB), www.swissadme.ch (accessed February 13, 2017).

(35) QikProp Schrödinger Release 2015-1: QikProp, Schrödinger, LLC, New York, NY, 2017 (accessed February 20, 2017).

(36) Lipinski, C. A.; Lombardo, F.; Dominy, C. A.; Feeney, P. J.. Experimental and computational approaches to estimate solubility and permeability in drug discovery and development settings. *Adv. Drug. Delivery Rev.* **2001**, *46*, *3*-26.

(37) Pajouhesh, H.; Lenz, G. R. Medicinal chemical properties of successful central nervous system drugs. *NeuroRx* **2015**, *2*, 541-553.

(38) Moriguchi, I.; Hirono, S.; Liu, Q.; Nakagome, I.; Matsushita, Y. Simple method of calculating octanol/water partition coefficient. Chem. *Pharm. Bull.* **1992**, *40*, 127-130.

(39) Moriguchi, I.; Hirono, S.; Liu, Q.; Nakagome, I.; Hirano, H. Comparison of reliability of log P values for drugs calculated by several methods. *Chem. Pharm. Bull.* **1994**, *42*, 976-978.

(40) *Clarity* software, DataApex, Prague, The Czech Republic, 2016.

(41) Jasco, Ishikawa-cho, Hachioji City, Tokyo, Japan.

(42) *PyMOL* version1.2r1. DeLanoScientificLLC: San Carlos, CA, 2009.

(43) Berman, H. M.; Westbrook, J.; Feng, Z.; Gilliland, G.; Bhat, T. N.; Weissig, H.; Shindyalov, I. N.; Bourne, P. E. The Protein Data Bank. *Nucleic Acids Res.* **2000**, *28*, 235-242.

(44) Zhao, Z.; Wolkenberg, S. E.; Lu, M.; Munshi, V.; Moyer, G.; Feng, M.; Carella, A.V.; Ecto, L. T.; Gabryelski, L. J.; Lai, M. T.; Prasad, S. G.; Yan, Y.; McGaughey, G. B.; Miller, M. D.; Lindsley, C. W.; Hartman, G. D.; Vacca, J. P.; Williams, T. M. Novel indole-3-sulfonamides as potent HIV non-nucleoside reverse transcriptase inhibitors (NNRTIs). *Bioorg. Med. Chem. Lett.* **2008**, *18*, 554-559.

(45) Lansdon, E. B.; Brendza, K. M.; Hung, M.; Wang, R.; Mukund, S.; Jin, D.; Birkus, G.; Kutty, N.; Liu, X. Crystal structures of HIV-1 reverse transcriptase with etravirine (TMC125) and rilpivirine (TMC278): implications for drug design. *J. Med. Chem.* **2010**, *53*, 4295-4299.

(46) Das, K.; Ding, J.; Hsiou, Y.; Clark, A. D. Jr.; Moereels, H.; Koymans, L.; Powels, R.; Janssen, P. a.; Boyer, P. L.; Clark, P.; Smith, R. H. Jr.; Kroeger Smith, M. B.; Micheida, C. J.; Hughes, S. H.; Arnold, E. Crystal structures of 8-Cl and 9-Cl TIBO complexed with wild-type HIV-1 RT and 8-Cl TIBO complexed with the Tyr181Cys HIV-1 RT drug-resistant mutant. *J. Mol. Biol.* **1996**, *264*, 1085-1100.

(47) *Molecular Operating Environment (MOE),* 2009.10. Chemical Computing Group Inc., 1010 Sherbooke St. West, Suite #910, Montreal, QC, Canada, H3A 2R7.

(48) Korb, O.; Stützle, T.; Exner, T. E. An ant colony optimization approach to flexible protein-ligand docking. *Swarm Intell.* **2007**, *1*, 115-134.

(49) Case, D. A.; Cheatham, T. E. 3rd; Darden, T.; Gohlke, H.; Luo, R.; Merz, K. M. Jr.; Onufriev, A.; Simmerling, C.; Wang, B.; Woods, R. J. The Amber biomolecular simulation programs. *J. Comp. Chem.* **2005**, *26*, 1668-1688.

(50) Wang, J.; Wang, W.; Kollman, P. A.; Case, D. A. Automatic atom type and bond type perception in molecular mechanical calculations. *J. Mol. Graph. Model.* **2006**, *25*, 247-260.

(51) Wang, J.; Wolf, R. M.; Caldwell, J. W.; Kollman, P.A.; Case, D.A. Development and testing of a general amber force field. *J. Comp. Chem.* **2004**, *25*, 1157-1174.

(52) Roe, D. R.; Cheatham, T. E. 3rd. *PTRAJ and CPPTRAJ:* Software for processing and analysis of molecular dynamics trajectory data. *J. Chem. Theor. Comp.* **2013**, *9*, 3084-3095.

(53) Cui, Q.; Sulea, T.; Schrag, J. D.; Munger, C.; Hung,M.-N.; Naïm, M., Cygler, M.; Purisima, E. O. Molecular dynamics and solvated interaction energy studies of protein-protein interactions: the MP1-p14 scaffolding complex. *J. Mol. Biol.* **2008**, *379*, 787-802.

(54) Naïm, M.; Bhat, S.; Rankin, K. N.; Dennis, S.; Chowdhury, S. F.; Siddiqi, I.; Drabik, P.; Sulea, T.; Bayly, C.; Jakalian, A.; Purisima, E. O. Solvated interaction energy (SIE) for scoring

protein-ligand binding affinities. 1. Exploring the parameter space. *J. Chem. Inf. Model.* **2007**, *47*, 122-133.

(55) Badia, R.; Grau, J.; Riveira-Muñoz, E.; Ballana, E.; Giannini, G.; Esté, J. A. The thioacetate-ω(γ-lactam carboxamide) HDAC inhibitor ST7612AA1 as HIV-1 latency reactivation agent. *Antiviral Res.* **2015**, *123*, 62-69.

(56) Maga, G.; Amacker, M.; Ruel, N.; Hubsher, U.; Spadari, S. Resistance to nevirapine of HIV-1 reverse transcriptase mutants: loss of stabilizing interactions and thermodynamic or steric barriers are induced by different single amino acid substitutions. *J. Mol. Biol*. **1997**, *274*, 738-747.

(57) Lauro, C.; Cipriani, R.; Catalano, M.; Trettel, F.; Chece, G.; Brusadin, V.; Antonilli, L.; van Rooijen, N.; Eusebi, F.; Fredholm, B. B.; Limatola, C. Adenosine A1 receptors and microglial cells mediate CX3CL1-induced protection of hippocampal neurons against Glu-induced death. *Neuropsychopharm.* **2010**, *35*, 1550-1559.

(58) Volontè, C.; Ciotti, M. T.; Battistini, L. Development of a method for measuring cell number: application to CNS primary neuronal cultures. *Cytometry* **1994**, *17*, 274-276.

(59) Lauro, C.; Di Angelantonio, S.; Cipriani, R.; Sobrero, F.; Antonilli, L.; Brusadin, V.; Ragozzino, D.; Limatola, C .Activity of adenosine receptors type 1 Is required for CX3CL1-mediated neuroprotection and neuromodulation in hippocampal neurons. *J. Immunol.* **2008**, *180*, 7590-7596.

TOC GRAPHIC

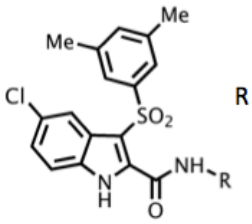

R =

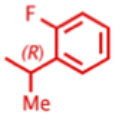

(*R*)-**8**

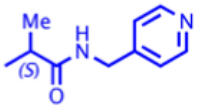

(*S*)-**23**

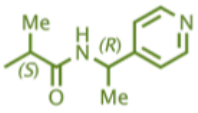

(*S,R*)-**25**

EC_{50} (nM)	(*R*)-**8**	(*S*)-**8**	(*S*)-**23**	(*R*)-**23**	(*S,R*)-**25**	(*R,S*)-**25**
HIV-1 WT	0.7	0.7	0.7	0.7	0.6	1.9 ± 0.4
K103N	0.7	103	0.7	114 ± 4	0.6	204 ± 37
Y181C	0.7	680 ± 432	0.7	181 ± 38	0.6	668 ± 37
Y188L	165 ± 21	>51551	666 ± 38	>23104	742 ± 260	>28532

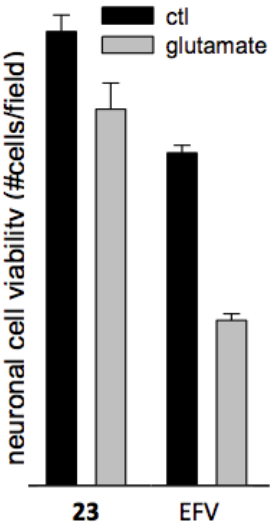

Supporting Information

Chiral Indolylarylsulfone Non-Nucleoside Reverse Transcriptase Inhibitors as New Potent and Broad Spectrum anti-HIV-1 Activity Agents

Valeria Famiglini, Giuseppe La Regina, Antonio Coluccia, Domiziana Masci, Andrea Brancale, Roger Badia, Eva Riveira-Muñoz, José A. Esté, Emmanuele Crespan, Alessandro Brambilla, Giovanni Maga, Myriam Catalano, Cristina Limatola, Francesca Romana Formica, Roberto Cirilli, Ettore Novellino, and Romano Silvestri

Contents of SI

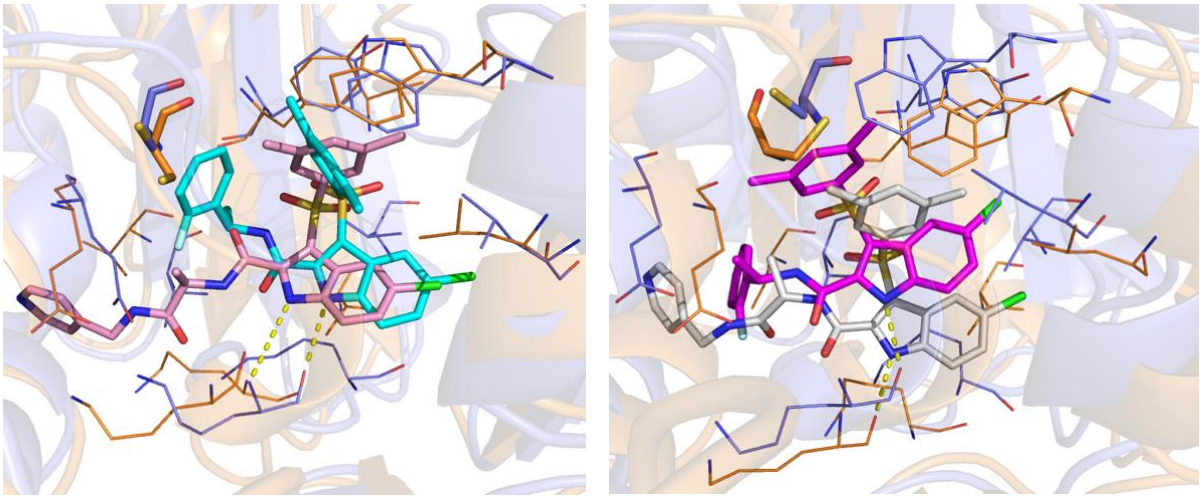

Figure 1S. Left panel: trajectories snapshots of (*R*)-**8** and (*R*)-**23** versus Y181C RT. Right panel: trajectories snapshots of (*S*)-**8** with (*S*)-**23** versus Y181C RT. Residues involved in interactions are reported as lines. Mutated residue is depicted as stick. RT is shown as cartoon. H-bonds are depicted as yellow dotted lines.

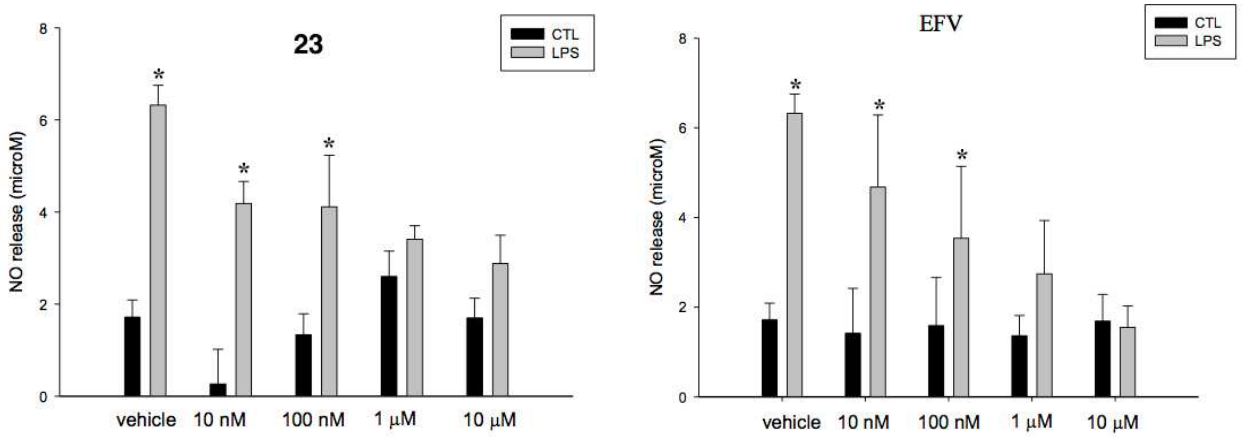

Figure 2S. Compound **23** and EFV treatments reduce NO release induced by LPS on BV2 cells. BV2 cells were treated with 10 nM, 10^2 nM, 10^3 nM or 10^4 nM concentrations of **23** or EFV in the presence or absence of 50 ng/mL LPS for 24 h. NO release was measured by Greiss reaction. Data are expressed as μM. N=3; *p<0,05 vs CTL by Kruskal-Wallis One Way Analysis of Variance (Dunn's method).

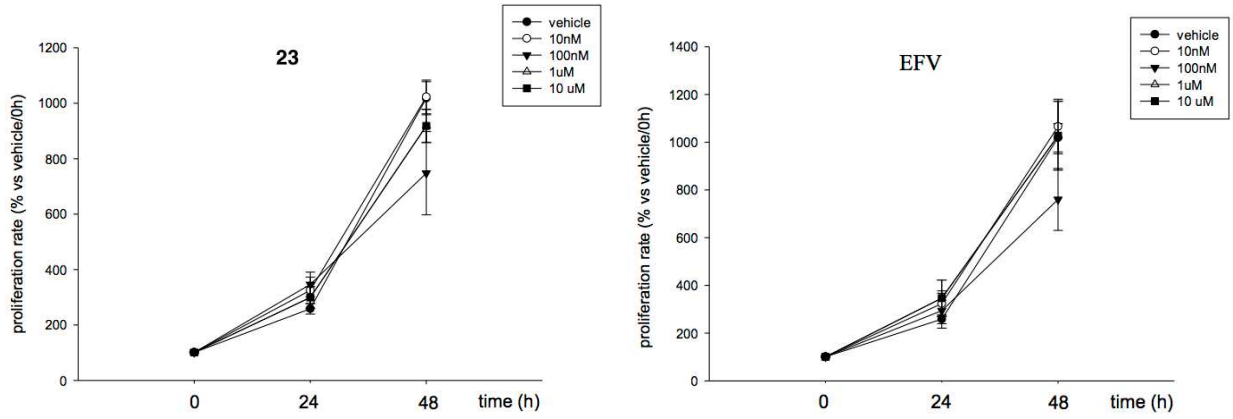

Figure 3S. Compound **23** and EFV treatments do not modify BV2 cell proliferation. BV2 cells were treated with 10 nM, 10^2 nM, 10^3 nM and 10^4 nM of **23** or EFV for 0, 24 and 48 h. Proliferation rate was measured by MTT assay. Data are expressed as % vs vehicle at 0h. N=3.

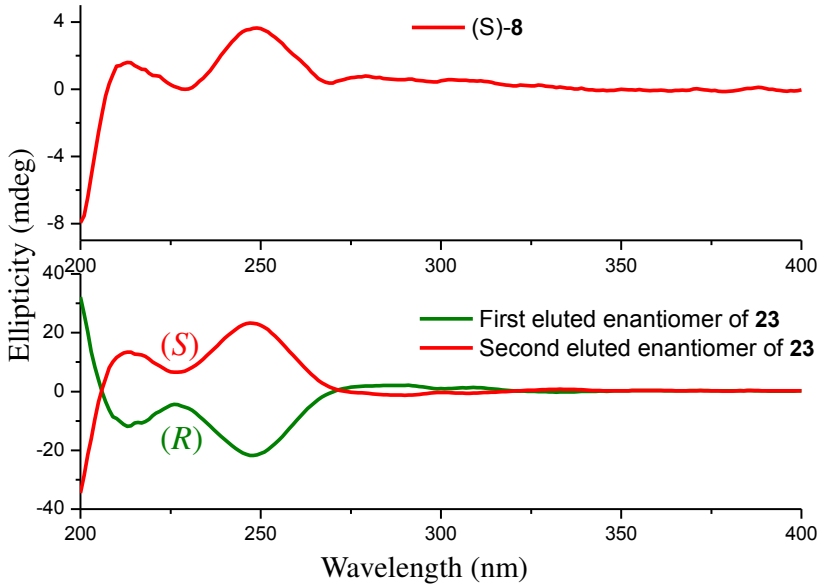

Figure 4S. Comparison of the CD spectra of (*S*)-**8** and the enantiomers of **23** recorded in ethanol.

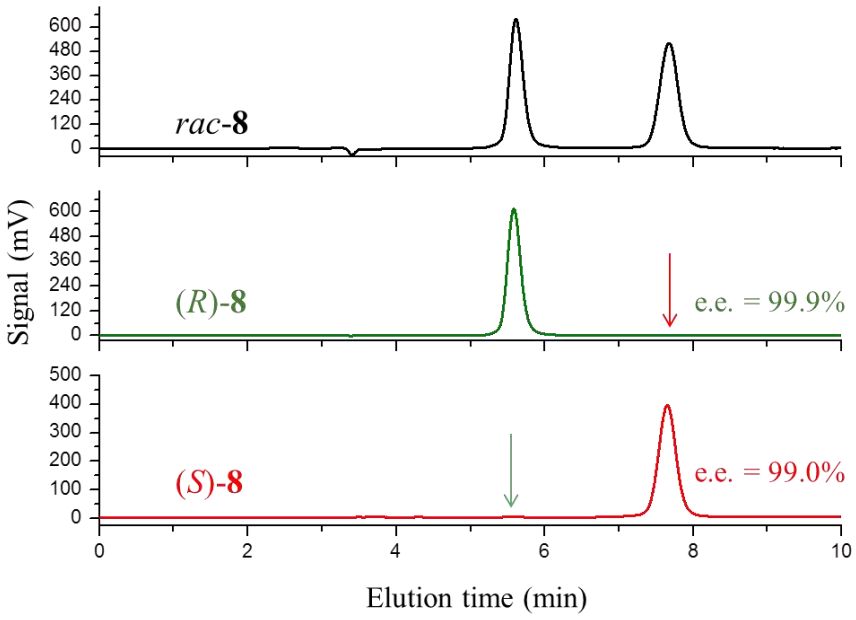

Figure 5S. Enantiomeric purity of the enantiomers of **8** separated at semipreparative scale.

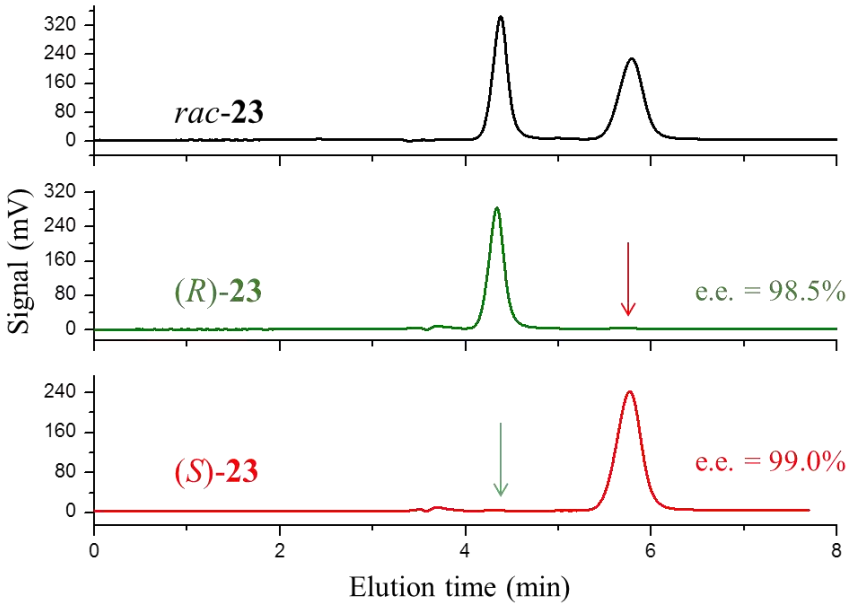

Figure 6S. Enantiomeric purity of the enantiomers of **23** separated at semipreparative scale.

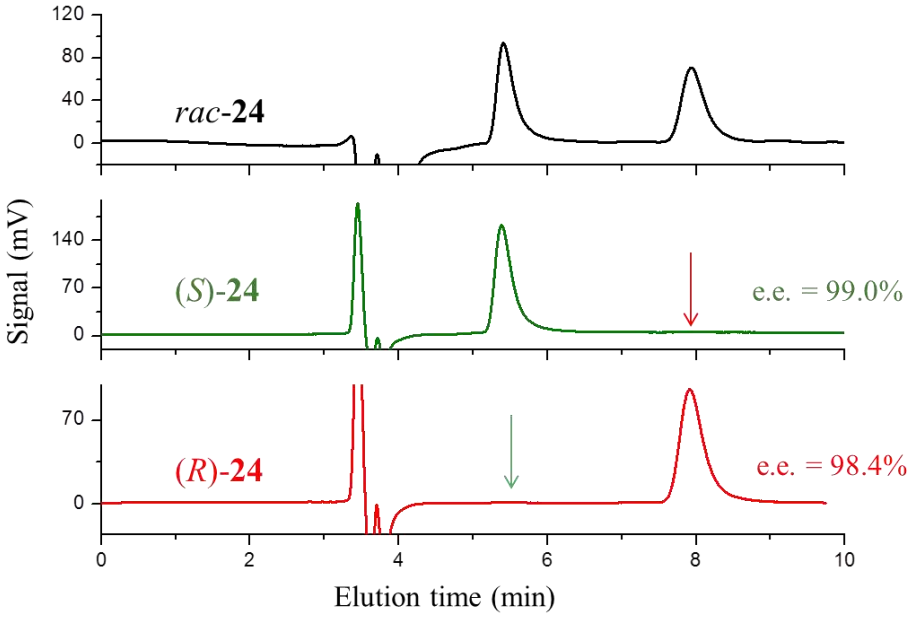

Figure 7S. Enantiomeric purity of the enantiomers of **24** separated at semipreparative scale.

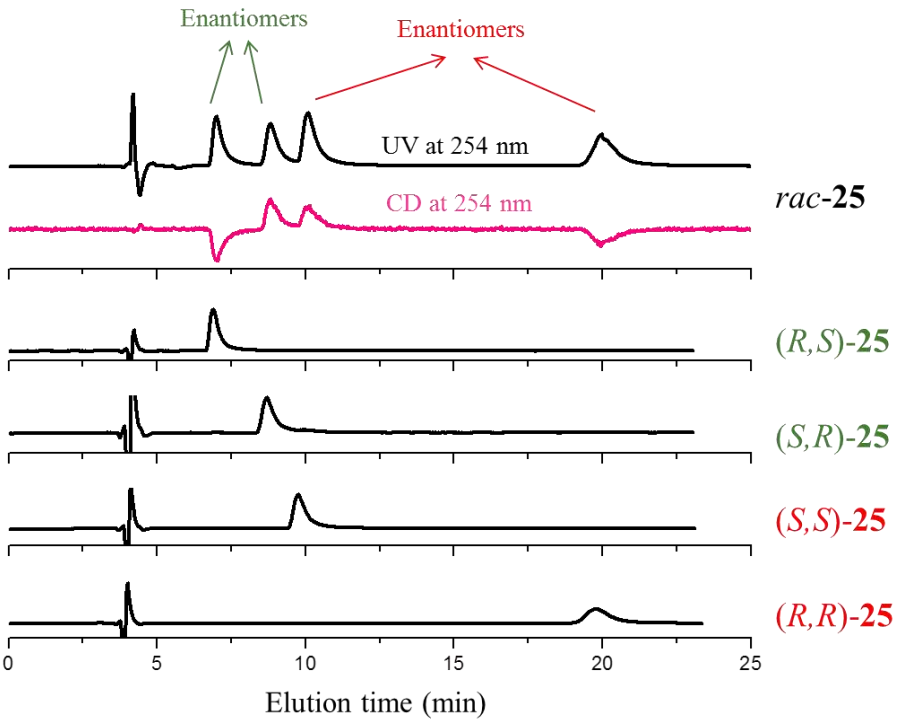

Figure 8S. Enantiomeric purity of the enantiomers of **25** separated at semipreparative scale.

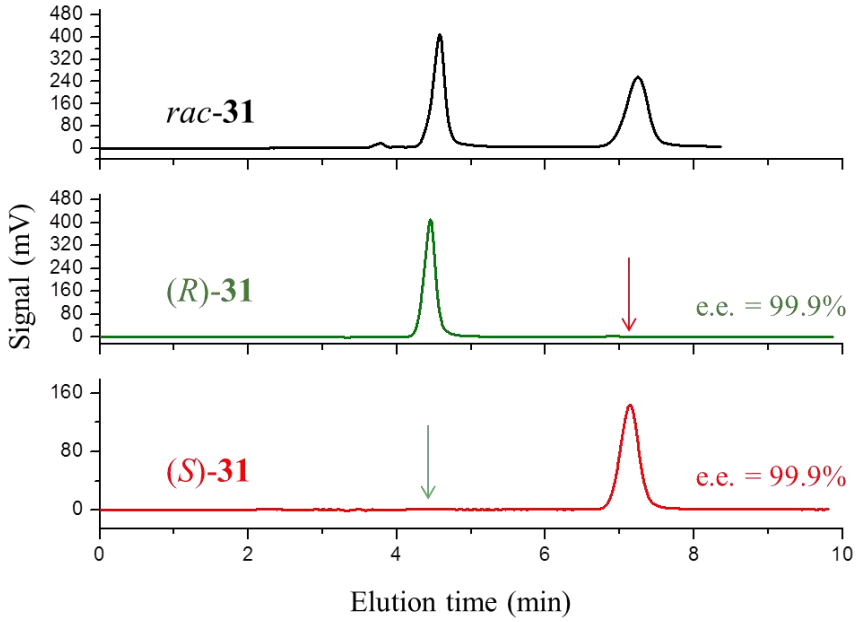

Figure 9S. Enantiomeric purity of the enantiomers of **31** separated at semipreparative scale.

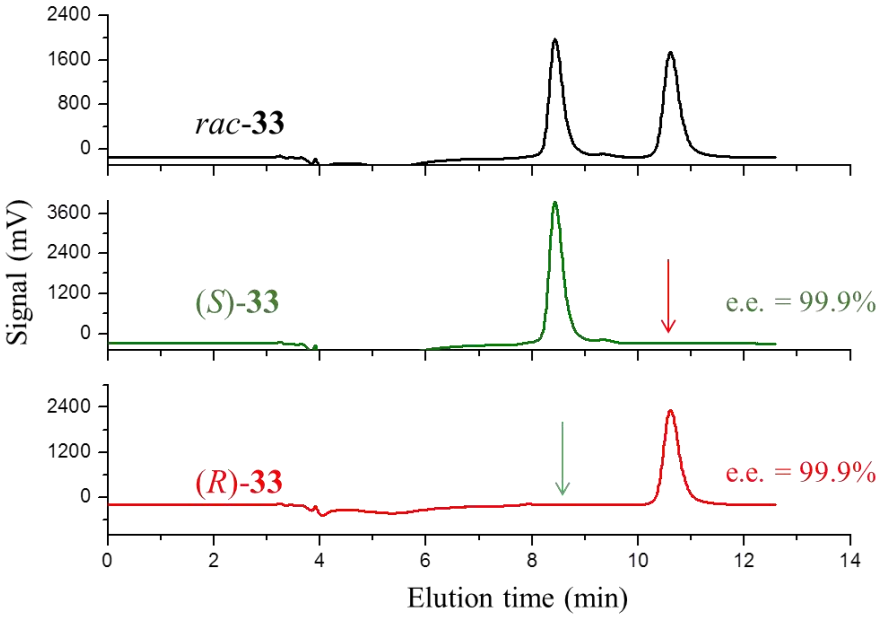

Figure 10S. Enantiomeric purity of the enantiomers of **33** separated at semipreparative scale.

Table 1S. In silico physicochemical properties of **9-22, 24** and **26-37**.

Cmpd	LogP[a]	TPSA[b]	H-bond Acc.[c]	H-bond Don.[d]	MW[e]	QPP Caco[f]	QPP MDCK[g]
9	2.70	100.55	4	2	456.94	1359.11	1719.66
10	4.75	87.41	3	2	527.46	1390.83	4295.93
11	3.71	96.64	5	2	500.97	1702.21	3131.21
12	4.62	87.41	5	2	502.96	1430.99	5407.89
13	3.99	87.41	4	2	484.97	1184.16	2460.85
14	4.42	87.41	5	2	488.94	1093.77	3640.43
15	2.00	124.09	5	2	478.95	148.66	153.92
16	2.00	124.09	5	2	478.95	131.72	134.9
17	3.14	113.43	3	3	467.97	275.47	299.61
18	2.97	142.11	4	4	507.99	74.95	74.46
19	3.22	116.09	4	3	492.98	378.62	431.52
20	3.01	116.51	4	3	524.04	305.67	603.56
21	3.21	116.51	4	3	538.08	555.98	882.22
22	1.82	129.40	5	3	511.00	140.77	269.22
24	2.03	129.40	5	3	525.03	214.84	388.32
26	2.65	144.75	4	3	530.07	235.21	725.6
27	2.85	144.75	4	3	544.10	347.91	1050.92
28	1.50	180.15	7	3	573.03	301.56	943.23
29	1.70	180.15	7	3	587.05	190.26	201.45
30	1.25	141.29	6	3	511.99	135.68	258.24
31	1.45	142.29	6	3	526.02	176.09	279.78
32	1.65	129.65	5	3	499.98	197.37	372.13
33	1.86	129.65	5	3	514.00	277.73	554.97
34	3.18	116.51	5	3	528.00	240.43	688.91
35	3.38	116.51	5	3	542.03	464.70	1224.57
36	3.38	116.51	5	3	542.03	400.35	860.26
37	3.57	116.51	5	3	556.06	627.59	1446.23

Physicochemical properties predicted by SwissADME:[1S] [a]Octanol-water partition coefficient predictor by topological method implemented from Moriguchi;[2S,3S] [b]Molecular polar surface area: this parameter correlates with human intestinal absorption (<140).[4S] [c]Number of H-bond acceptors; [d]Number of H-bond donors; [e]Molecular Weight. Physicochemical properties predicted by QikProp:[5S] [f]QPP Caco - Apparent Caco-2 permeability (nm/sec) (<25 poor, >500 great); [g]QPP MDCK - Apparent MDCK permeability (nm/sec) (<25 poor, >500 great).

Table 2S. Elemental analyses of compounds 8-37.

compd	Calculated (%)	Found (%)
8	C, 61.91; H, 4.57; Cl, 7.31; F, 3.92; N, 5.78; S, 6.61	C, 61.76; H, 4.52; Cl, 7.11; F, 3.80; N, 5.62; S, 6.42
9	C, 60.46; H, 4.63; Cl, 7.76; N, 6.13; S, 7.02	C, 60.25; H, 4.59; Cl, 7.62; N, 6.02; S, 6.88
10	C, 61.48; H, 4.59; Cl, 13.44; N, 5.31; S, 6.08	C, 61.37; H, 4.54; Cl, 13.36; N, 5.22; S, 5.90
11	C, 59.94; H, 4.43; Cl, 7.08; F, 3.79; N, 5.59; S, 6.40	C, 59.85; H, 4.39; Cl, 6.91; F, 3.65; N, 5.48; S, 6.32
12	C, 59.70; H, 4.21; Cl, 7.05; F, 7.55; N, 5.57; S, 6.38	C, 59.59; H, 4.17; Cl, 6.88; F, 7.37; N, 5.68; S, 6.19
13	C, 61.91; H, 4.40; Cl, 7.31; F, 3.92; N, 5.78; S, 6.61	C, 61.84; H, 4.44; Cl, 7.19; F, 3.75; N, 5.69; S, 6.48
14	C, 58.96; H, 3.92; Cl, 7.25; F, 7.77; N, 5.73; S, 6.56	C, 58.68; H, 3.88; Cl, 7.13; F, 7.58; N, 5.61; S, 6.88
15	C, 59.42; H, 3.69; Cl, 7.63; N, 12.05; S, 6.90	C, 59.26; H, 3.61; Cl, 7.40; N, 11.95; S, 6.78
16	C, 59.42; H, 3.69; Cl, 7.63; N, 12.05; S, 6.90	C, 59.34; H, 3.61; Cl, 7.51; N, 11.88; S, 6.71
17	C, 61.60; H, 4.74; Cl, 7.58; N, 8.98; S, 6.85	C, 61.50; H, 4.68; Cl, 7.48; N, 8.81; S, 6.78
18	C, 59.11; H, 4.37; Cl, 6.98; N, 13.79; S, 6.31	C, 58.89; H, 4.32; Cl, 6.88; N, 13.68; S, 6.20
19	C, 60.51; H, 4.46; Cl, 7.24; N, 11.44; S, 6.55	C, 60.42; H, 4.42; Cl, 7.13; N, 11.29; S, 6.31
20	C, 61.88; H, 5.00; Cl, 6.77; N, 8.02; S, 6.12	C, 61.73; H, 4.98; Cl, 6.64; N, 7.92; S, 5.97
21	C, 62.50; H, 5.25; Cl, 6.59; N, 7.81; S, 5.96	C, 62.42; H, 5.16; Cl, 6.42; N, 7.70; S, 5.85
22	C, 58.76; H, 4.54; Cl, 6.94; N, 10.96; S, 6.28	C, 58.59; H, 4.48; Cl, 6.78; N, 10.82; S, 6.07
23	C, 59.48; H, 4.80; Cl, 6.75; N, 10.67; S, 6.11	C, 59.31; H, 4.72; Cl, 6.69; N, 10.58; S, 5.93
24	C, 59.48; H, 4.80; Cl, 6.75; N, 10.67; S, 6.11	C, 59.26; H, 4.71; Cl, 6.66; N, 10.39; S, 5.90
25	C, 60.16; H, 5.05; Cl, 6.58; N, 10.39; S, 5.95	C, 59.98; H, 4.99; Cl, 6.42; N, 10.25; S, 5.72
26	C, 56.65; H, 4.56; Cl, 6.69; N, 7.93; S, 12.10	C, 56.51; H, 4.49; Cl, 6.45; N, 7.81; S, 11.95
27	C, 57.40; H, 4.82; Cl, 6.52; N, 7.72; S, 11.79	C, 57.27; H, 4.80; Cl, 6.48; N, 7.52; S, 11.54
28	C, 52.40; H, 4.40; Cl, 6.19; N, 14.67; S, 5.60	C, 52.12; H, 4.34; Cl, 5.98; N, 14.42; S, 5.46
29	C, 53.19; H, 4.64; Cl, 6.04; N, 14.32; S, 5.46	C, 53.04; H, 4.58; Cl, 5.89; N, 14.15; S, 5.21
30	C, 56.30; H, 4.33; Cl, 6.92; N, 13.68; S, 6.26	C, 56.21; H, 4.29; Cl, 6.78; N, 13.38; S, 6.07
31	C, 57.08; H, 4.60; Cl, 6.74; N, 13.31; S, 6.10	C, 56.91; H, 4.52; Cl, 6.51; N, 13.05; S, 5.88
32	C, 57.66; H, 4.44; Cl, 7.09; N, 8.40; S, 6.41	C, 57.48; H, 4.37; Cl, 6.95; N, 8.21; S, 6.25
33	C, 58.42; H, 4.71; Cl, 6.90; N, 8.18; S, 6.24	C, 58.25; H, 4.68; Cl, 6.75; N, 7.92; S, 6.11
34	C, 59.14; H, 4.39; Cl, 6.71; F, 3.60; N, 7.96; S, 6.07	C, 58.92; H, 4.28; Cl, 6.64; F, 3.49; N, 7.72; S, 5.87
35	C, 59.83; H, 4.65; Cl, 6.54; F, 3.51; N, 7.75; S, 5.92	C, 59.55; H, 4.59; Cl, 6.28; F, 3.42; N, 7.51; S, 5.70
36	C, 59.83; H, 4.65; Cl, 6.54; F, 3.51; N, 7.75; S, 5.92	C, 59.61; H, 4.54; Cl, 6.37; F, 3.40; N, 7.49; S, 5.78
37	C, 60.48; H, 4.89; Cl, 6.38; F, 3.42; N, 7.56; S, 5.77	C, 60.37; H, 4.82; Cl, 6.25; F, 3.28; N, 7.38; S, 5.41

References of Supporting Information

(1S) SwissADME website for computation of physicochemical descriptors and ADME parameterrs prediction, Swiss Institute of Bioinformatics (SIB), www.swissadme.ch.

(2S) Moriguchi, I.; Hirono, S.; Liu, Q.; Nakagome, I.; Matsushita, Y. Simple method of calculating octanol/water partition coefficient. Chem. *Pharm. Bull.* **1992** 40, 127-130.

(3S) Moriguchi, I.; Hirono, S.; Liu, Q.; Nakagome, I.; Hirano, H. Comparison of reliability of log P values for drugs calculated by several methods. *Chem. Pharm. Bull.* **1994** 42, 976-978.

(4S) Pajouhesh, H.; Lenz, G. R. Medicinal chemical properties of successful central nervous system drugs. NeuroRx **2015**, *2*, 541-553.

(5S) QikProp Schrödinger Release 2015-1: QikProp, Schrödinger, LLC, New York, NY, 2017.